Acta Scientiarum
http://periodicos.uem.br/ojs
ISSN on-line: 1807-8664
Doi: 10.4025/actascitechnol.v43i1.50263

Adsorption of Cd (II), Pb (II) and Cr (III) on chemically modified *Euterpe Oleracea* biomass for the remediation of water pollution

Affonso Celso Gonçalves Junior[1], Daniel Schwantes[2*], Elio Conradi Junior[3], Juliano Zimmermann[1] and Gustavo Ferreira Coelho[1]

[1]Universidade Estadual do Oeste do Paraná, Marechal Cândido Rondon, Paraná, Brazil. [2]Departamento de Ciências Vegetais, Faculdade de Agronomia e Ingeniería Florestal, Pontificia Universidade Católica do Chile, Avenida Vicuña Mackenna, 4860, 7820436, Macul, Santiago, Chile. [3]Programa de Pós-Graduação em Agronomia, Universidade Estadual do Oeste do Paraná, Marechal Cândido Rondon, Paraná, Brazil. *Author for correspondence. E-mail: daniel_schwantes@hotmail.com

ABSTRACT. This study evaluated the use of *Euterpe oleracea* endocarp after chemical modification with H_2O_2, H_2SO_4 and NaOH for the removal of Cd^{2+}, Pb^{2+} and Cr^{3+} from water. Therefore, the adsorbent was characterized for its chemical composition, Fourier Transform Infrared (FTIR) analysis, Scanning Electron Microscope (SEM) images, and pH of point of zero charge (pH_{PZC}), thermal stability and porosimetry. Adsorption tests were conducted by using a Central Composite Design (CCD). Pseudo-first order, pseudo-second order, Elovich and intraparticle diffusion models evaluated the adsorption kinetics, and sorption isotherms were linearized according to Langmuir, Freundlich and Dubinin-Radushkevich. The effect of initial concentration, temperature in the process and the desorption were also analyzed. SEM results showed that the *açaí* adsorbents (or CA) had irregular and heterogeneous structure, and IR analysis evidenced the presence of hydroxyl, aliphatic, phenolic and carboxylic surface groups; both analyses indicate favorable adsorption characteristics. The pH_{PZC} of the adsorbent is 4.41, 4.02 and 7.10 for CA modified with H_2O_2, H_2SO_4 and NaOH, respectively. The optimum adsorption conditions were pH 5.0, within 40 min, with 4 g L^{-1} as the ideal adsorbent dose. The predominance of chemisorption occurs, in mono and multilayer. The adsorption is only spontaneous for Cd^{2+} at 15 and 25°C. The CA has the potential to increase the removal efficiency of Cd, Pb and Cr, when chemically modified, particularly with H_2O_2 and H_2SO_4.

Keywords: biosorption, water contamination, metals adsorption, water treatment.

Received on October 11, 2019.
Accepted on February 13, 2020.

Introduction

The release of toxic elements into the environment is often caused by impacts of different agricultural and industrial activities. Metals originating from human activities are frequently detected in the environmental compartments; such as sediment, rivers, lakes, among others, causing severe contamination in water bodies (Schiller et al., 2019). The metal contamination in aquatic environments is worrisome because of its toxicity, abundance, permanence in the environment, and subsequent accumulation in aquatic habitats, microorganisms, aquatic flora and fauna, can enter the food chain and cause significant effects on human health in the long term (Conradi Jr. et al., 2019).

According to Schwantes et al. (2019), the efficient removal of metal ions and pesticides from wastewater has become an important issue. Some methods, such as precipitation, followed by coagulation and membrane filtration, have been used to remove metals from water. However, these processes become unfeasible due to the production of sludge, low metals removal, and high cost, thus limiting the practical use. Among the various methods, the adsorption process is an effective method used to remove toxic metals from aqueous solution (Conradi Jr. et al., 2019). The search for new adsorbents has been focused on biomaterials, because they are economically viable, biodegradable, and derived from renewable resources. In general, these materials are locally and easily available at large amounts; also, they are inexpensive and have little economic value (Cutillas-Barreiro et al., 2014; Quintáns-Fondo et al., 2016).

The agribusiness is one of the main generators of waste with adsorbing potential for various contaminants. Among the diversity of crops in Brazil that can be used for this purpose, stands out the *E. oleracea* crop, a native Brazilian tropical palm tree, found in the North and Northeast of the country. The main production of *E. oleracea* is for juices, and in this process, approximately 80% of the total volume of waste consists of endocarp or seed of *E. oleracea* (Pacheco-Palencia, Duncan, & Talcott, 2009; Nascimento, Cicero, & Novembre, 2010).

Several studies demonstrate promising results in using biosorbents for removal or adsorption of metals. Such as *Moringa oleifera* Lam. (Gonçalves Jr. et al., 2013a; Meneghel et al., 2013), *Crambe abyssinica* Hochst (Gonçalves Jr. et al., 2013b; Rubio et al., 2013a; 2013b), cassava industry waste (Schwantes, Gonçalves Jr., Strey, Schwantes, & Nacke, 2013), *Jatropha curcas* biomass (Nacke et al., 2016), pinus barks (Schwantes et al., 2018a) and cashew nut shell (Coelho et al., 2014).

However, according to Schwantes et al. (2018a), in order to increase the sorption potential of natural adsorbents, through the formation of new functional groups on the surface of the adsorbent, several studies report the use of chemical alterations in adsorbents, especially those of plant origin (Schwantes et al., 2015; 2016).

The removal of metals from contaminated waters using *E. Oleracea* wastes has been already studied by Gonçalves Jr. et al. (2016) with good results and perspectives, but only as a biosorbent. But we do not know very much about the effectiveness in this material after chemical modifications yet. Besides, any attempt to technify or improve the productive chain of an Amazon fruit is mostly welcome, because this may represent a possibility of sustainable development to the Amazon Region, helping to simultaneously develop and preserve the biodiversity and the tropical forest.

Thus, this study aimed (i) to evaluate the efficiency of chemically modified *E. Oleracea* endocarp in the removal of Cd^{2+}, Pb^{2+} and Cr^{3+} from contaminated solutions, and (ii) to study the adsorption mechanism of interaction between the *E. Oleracea* based adsorbents and the evaluated metal ions.

Material and methods

Preparation of modified adsorbents

The *Euterpe oleracea* M. endocarps were obtained in the city of Curinópolis, Pará State, located in the North region of Brazil (Amazonia). As one of the main common names for this fruit in Brazil is *Açaí*, and the common name for its solid wastes is *Cascas de Açaí* or açaí barks, so, we named the biosorbent from *Euterpe oleracea* M. as CA.

The experiment was conducted in the Laboratory of Environmental and Instrumental Chemistry of the State University of Western Paraná - Unioeste, campus Marechal Cândido Rondon.

The waste material was dried at 60°C for 48 hours. After drying, the wastes were sieved through 14 and 65 mesh aimed standardizing the size of particles to 0.212-1.40 mm and obtaining the fresh material (biosorbent). The chemical modifications were carried out by immersing the fresh adsorbent in solutions of 1.0 mol L^{-1} H_2O_2, H_2SO_4 and NaOH, 1:10 (m v^{-1}) under constant stirring at 150 rpm at 60°C for 6 hours. Then, the modified adsorbents were washed in ultrapure water to remove the excess of the modifying solution and, after that, they were dried at 60°C until constant weight.

Material characterization

The concentration of total elements (K, Ca, Mg, Cu, Fe, Mn, Zn, Cd, Pb and Cr) was determined by nitroperchloric digestion (Latimer, 2012), with latter concentration determination by means of flame atomic absorption spectrometry (FAAS), using curves with certified standards for all metals (GBC 932 AA). The surface morphology of the material was evaluated by scanning electron microscopy (SEM) using a JEO JSM 6360-LV microscope, equipped with dispersive energy microscopy.

The main functional groups in the adsorbents were also determined by infrared spectroscopy (IR), in a FTIR-8300 Fourier Transform spectrometer (Shimadzu Infrared Spectrophotometer) in the region between 400 to 4000 cm^{-1}, with 4 cm^{-1} resolution, whose transmittance spectra was obtained using KBr pellets. The determination of the zero-charge point (pH_{PZC}) of the adsorbent was conducted using the methodology adapted from Mimura, Vieira, Martelli, and Gorgulho (2010). In order to verify the thermal stability of the adsorbent mass, thermal analyses were carried out using a thermogravimetric analyzer (TGA 4000 Perkin

Elmer), where the samples were heated from 30 to 900˚C at a heating rate of 10°C min.$^{-1}$ under N^2 atmosphere. Aiming to check the accessibility of adsorbates inside the adsorbents, the specific surface area (SSA), volume and size of pore of the adsorbent materials were determined by using the equipment Quantachrome Nova 1200e. To this end, 500 mg material were heated to 200°C under vacuum for approximately 4 hours, followed by adsorption and desorption of nitrogen. The SSA and pore volume were calculated using a method adapted from the standard Brunauer, Emmett, and Teller (1938) and the pore size was obtained using a method adapted from Barrett, Joyner, and Halenda (1951).

Multivariate analysis for adsorbent dose and pH influence

The ideal conditions of adsorption were defined with the use of a Central Composite Design (CCD), testing five levels of mass (adsorbent doses) and pH levels using real values, coded, and three repetitions in the central value. Tests of adsorbent mass and pH were performed with five increasing values (250.0, 396.4, 750.0, 1103.6, 1250.0 mg) and five conditions of pH (3.0, 3.6, 5.0, 6.4 and 7.0), adjusted with HCl or NaOH solutions (0.1 mol L^{-1}) (Table 3). These values of mass and pH are combined with fixed volumes of 50 mL containing 10 mg L^{-1} monoelementar water solutions of Cd^{2+}, Pb^{2+} and Cr^{3+}, prepared from cadmium nitrate salts [$Cd(NO_3)_2 4H_2O$], lead nitrate [$Pb(NO_3)_2$], and nitrate of chromium (III) [$Cr(NO_3)_3\ 9H_2O$]. Following, they were stirred in thermostatic shaker (200 rpm at 25°C) for 90 min.

With the values obtained for final concentration, response surface graphics were constructed using the amount adsorbed of metals, calculated by Equation 1.

$$Qads = (C0 - Cf)\, m/V \quad (1)$$

where:
*Q*ads is the amount of metal ions adsorbed per gram of adsorbent at equilibrium (mg g^{-1});
m is the mass of adsorbent (g);
C_0 represents the initial concentration of ions in solution (mg L^{-1});
C_f is the concentration of ion in solution (mg L^{-1}) and;
V is the volume of used solution (L).

Adsorption kinetic mechanism

With the obtained results of adsorbent dose and pH from the previous tests, we determined the optimal time of sorption of metals. Thus, 200 mg of adsorbents were stirred for 12 different time intervals (5, 20, 30, 40, 50, 60, 80, 100, 120, 140, 160 and 180 min.) containing 50 mL monoelementar water solutions with 10 mg L^{-1} of metal at pH 5.0. Solutions were filtered through qualitative filter paper and the equilibrium concentration was determined by FAAS, which was used to estimate the kinetic mechanism that controls the adsorption process. The pseudo-first order (Lagergren, 1898) pseudo-second order (Ho & Mckay, 1999), Elovich (Roginski, 1948) and intraparticle diffusion (Weber & Morris, 1963) models were applied.

Adsorption and desorption efficiency, and the capacity of reusing the CA adsorbents

The experimental conditions of this step were based on the aforementioned results of dose, pH and equilibrium time obtained in the previous tests. Thus, 200 mg adsorbents containing 50 mL of 10 levels of monoelementar solutions of Cd^{2+}, Pb^{2+} and Cr^{3+} (5, 20, 40, 60, 80, 100, 120, 140, 160 and 200 mg) at pH 5.0, were stirred at 25°C and 200 rpm for 40 min. The solutions were filtered through qualitative filter paper and the equilibrium concentration was determined by FAAS. The Q_{ads} was calculated according to Equation 1 and the percentage of removal of metals was calculated by Equation 2.

$$\%R=100-(Ceq\times 100) \quad (2)$$

where:
%R is the percentage of removal of ion by adsorbent, and;
C_{eq} is the concentration of ion (mg L^{-1}) adsorbed.

In order to check the reuse capacity of the materials, the adsorbents used in the process were separated from the aqueous solution by filtration and oven-dried at 60°C for 24 hours. The mass of the adsorbent obtained after drying was disposed with 50 mL HCl solution (0.1 mol L^{-1}) and stirred for 40 min. (200 rpm at 25°C) to determine the final concentrations. Desorption percentage was calculated using Equation 3:

$$D=\left(\frac{Ceq(des)}{Ceq(ads)}\right) \times 100 \quad (3)$$

where:
$C_{eq(des)}$ (mg L^{-1}) and $C_{eq(ads)}$ (mg L^{-1}) are concentration desorbed, and the concentration adsorbed at equilibrium, respectively.

Adsorption isotherms

From the results obtained by the aforementioned studies, adsorption isotherms were determined by non-linear mathematical models of Langmuir, Freundlich and linear model Dubinin-Radushkevich (D-R), respectively presented in Equation 4, 5, 6, and 7.

$$q = \left(\frac{qmbC}{1 + bC}\right) \quad (4)$$

where:
q is the amount of solute adsorbed per unit of adsorbent mass (mg g^{-1});
q_m is a constant which represents the total number of available sites in the biosorbent material;
C is the equilibrium concentration of solute in the solution volume (mg L^{-1});
b is a constant that indicates the affinity of ion for sites in the adsorbent material (Langmuir, 1916).

$$Qe = K_f \times Ce^{1/n} \quad (5)$$

where:
C_e is the concentration at equilibrium and Q_e is the adsorbed amount at equilibrium per unit of adsorbent mass; K_F and n are the two parameters of Freundlich (1906).

$$lnQeq = lnQd - Bd\varepsilon^2 \quad (6)$$

where:
Q_{eq} is the amount of ion adsorbed per unit of adsorbent mass (mol g^{-1});
Q_d is the adsorption capacity (mol L^{-1});
B_d is a coefficient related to sorption energy (mol^2 J^{-2}) and 'ε' is the Polanyi potential.

$$\varepsilon = RTln\ (1 + 1/C_{eq}) \quad (7)$$

where:
R is the universal gas constant (kJ mol^{-1} K^{-1});
T is temperature (K) and C_{eq} is the equilibrium concentration in the liquid phase (mol L^{-1}) (Dubinin & Radushkevich, 1947).

Temperature influence

In order to check the influence of the temperature on adsorption, thermodynamic studies were performed. For this purpose, 200 mg of adsorbent material was added in 50 mL of solution containing 50 mg L^{-1} of Cd^{2+}, Pb^{2+} and Cr^{3+}, at pH 5.0, then shaken at 200 rpm at different temperatures (15, 25, 35, 45 and 55ºC).

From the obtained results the Gibbs free energy (ΔG), enthalpy (ΔH) and entropy (ΔS) were estimated, in order to evaluate the adsorption thermodynamics and investigate the nature of the process (Farghali, Bahgat, El Rouby, & Khedr, 2013).

Results and discussion

Characterization of the adsorbent materials

Total elements composition

The chemical characterization of the CA adsorbents is shown in Table 1, where it is possible to observe a reduction on the concentration of K (79%), Ca (82%), Mg (43%), Cu (58%), Zn (15%), Mn (43%), Fe (96%) and Pb (37%), for CA modified with NaOH.

Also it is observed a reduction of K (84%), Ca (84%), Mg (75%), Cu (24%), Zn (33%), Mn (99%), Fe (100%) and Pb (23%), for CA modified with H_2SO_4; and a reduction of K (71%), Ca (83%), Mg (61%), Cu (4%), Zn (9%), Mn (54%), Fe (92%) and Pb (3%), for CA modified with H_2O_2.

Table 1. Characterization of total elements in the fresh *açaí* endocarp (CA) and modified with H_2O_2, H_2SO_4 and NaOH.

Adsorbents	K	Ca	Mg	Cu	Zn	Mn	Fe	Cd	Pb	Cr
	g kg^{-1}			mg kg^{-1}						
Fresh CA	4.39	9.01	0.98	5.53	15.50	172.13	80.07	< LQ	15.30	< LQ
CA NaOH	0.91	1.64	0.56	2.30	13.20	98.10	3.10	< LQ	9.60	< LQ
CA H_2SO_4	0.70	1.43	0.24	4.20	10.40	2.10	< LQ	< LQ	11.70	< LQ
CA H_2O_2	1.26	1.53	0.38	5.30	14.10	78.20	6.20	< LQ	14.90	< LQ

LQ (Limit of Quantification): K = 0.01; Ca = 0.005; Mg = 0.005 (g kg^{-1}); Cu = 0.005; Fe = 0.01; Mn = 0.01; Zn = 0.005; Cd = 0.005; Pb = 0.01; Cr = 0.01 (mg kg^{-1}).

These changes/reductions are mostly caused by the contact/chemical reactions between the modifying agents (NaOH, H_2SO_4 and H_2O_2) and the structures and chemical composition of the lingo-cellulosic materials of *açaí*. It is important to point out that Cd and Cr were only detected in levels below the limits of quantification (LQ) of the used method.

As observed, the simple activation with NaOH can modify the surface of the fresh CA. As it is well known, sodium hydroxide when dissociated in water releases hydroxyl ions (OH^-), constituting a strong base with high corrosive power. That corrosion can destroy and/or modify the surface of the materials that is in contact with the base (Chazin, 2012).

Such results are perfectly understandable according to Bohli, Ouederni, Fiol, and Villaescusa (2015), because, as observed, the activating material significantly influences the characteristics of the final product. In addition, authors such as Schwantes et al. (2018a) brought up changes observed in the chemical composition after chemical modifications with H_2SO_4, NaOH and H_2O_2, in different vegetable biomass. Moreover, washing the material to neutral pH after the whole process may have contributed to the variation in the chemical composition of the adsorbents (Nacke et al., 2017; Schwantes, Gonçalves, Varennes, & Braccini, 2018b).

Scanning Electron Microscopy (SEM)

The microstructure of the fresh CA is observed under amplifications of 160x, 1200x and 12000x and the modified adsorbents under resolutions of 50x, 400x and 1600x (Figure 1). The surface of fresh CA, according to the Figure (1a, b, c), has fibrous and rough appearance with voids.

It is also possible to identify a laminar structure with crevices and pores in the surface, which are favorable characteristics for the adsorption of metal ions (Gonçalves Jr. et al., 2016). For CA modified with H_2O_2 (Figure 1d, e, f), it can be observed heterogeneity on the adsorbent surface in sponge shape, with pore-shaped fissures created by the oxidizing power of H_2O_2.

The dehydrating action of H_2SO_4 (1.0 mol L^{-1}) configured an irregular and heterogeneous surface, with many fissures (Figure 1g, h, i). As NaOH is a strong base of high solubility, it possibly caused irregular, heterogeneous surface and cavities (Figure 1j, k, l).

In fact, these characteristics assist in the adsorption of metals by increasing the surface area of the adsorbent. Some studies have already been conducted, such as described by Schwantes et al. (2016), which evidence the efficiency of metals adsorption using chemical pre-treatment of plant adsorbents from the agribusiness.

Infrared Spectroscopy (IS)

The infrared spectra for fresh CA adsorbent was obtained from previous studies (Gonçalves Jr. et al., 2016), which showed vibrational stretches in regions of 3442, 2923, 1735, 1631, 1517, 1440, 1380, 1247, 771 and 667 cm^{-1}. These vibrational stretches assigned to the presence of O-H bonds of hydroxyl groups (cellulose, lignin) and water adsorbed on the adsorbent surface, C-H of alkane groups and carbonyl groups (lignin and holocellulose), C-O bonds (amides and carboxylic groups), C-O stretch of phenols and the C-N bonds, respectively. According to Gonçalves Jr. et al. (2016), these groups favor the adsorption of metal ions.

The infrared spectra in the range 500-4000 cm^{-1} for the adsorbents modified with H_2O_2, H_2SO_4 and NaOH showed the presence of functional groups on the adsorbent surface (Figure 2).

In Figure 2, it is observed that materials modified with solutions of H_2O_2, H_2SO_4 and NaOH showed vibrational stretches in the region of 3382 and 3443 cm^{-1}, attributed to O-H bonds from primary amines and amides, carboxylic and hydroxylic acids found in lignin, cellulose and water (Pavia, Lampman, Kriz, & Vyvyan, 2010). The spectra in the region of 2922 cm^{-1}, attributed to C-H bonds of alkanes groups, aliphatic acids and aldehydes were also found in the three modified adsorbents. These groups have already been registered in other plant waste from agribusiness, such as cashew nut shell (Coelho et al., 2014), *Crambe abyssnica* H. meal (Rubio et al., 2013a; 2013b), *Jatropha curcas* L. meal (Nacke et al., 2016).

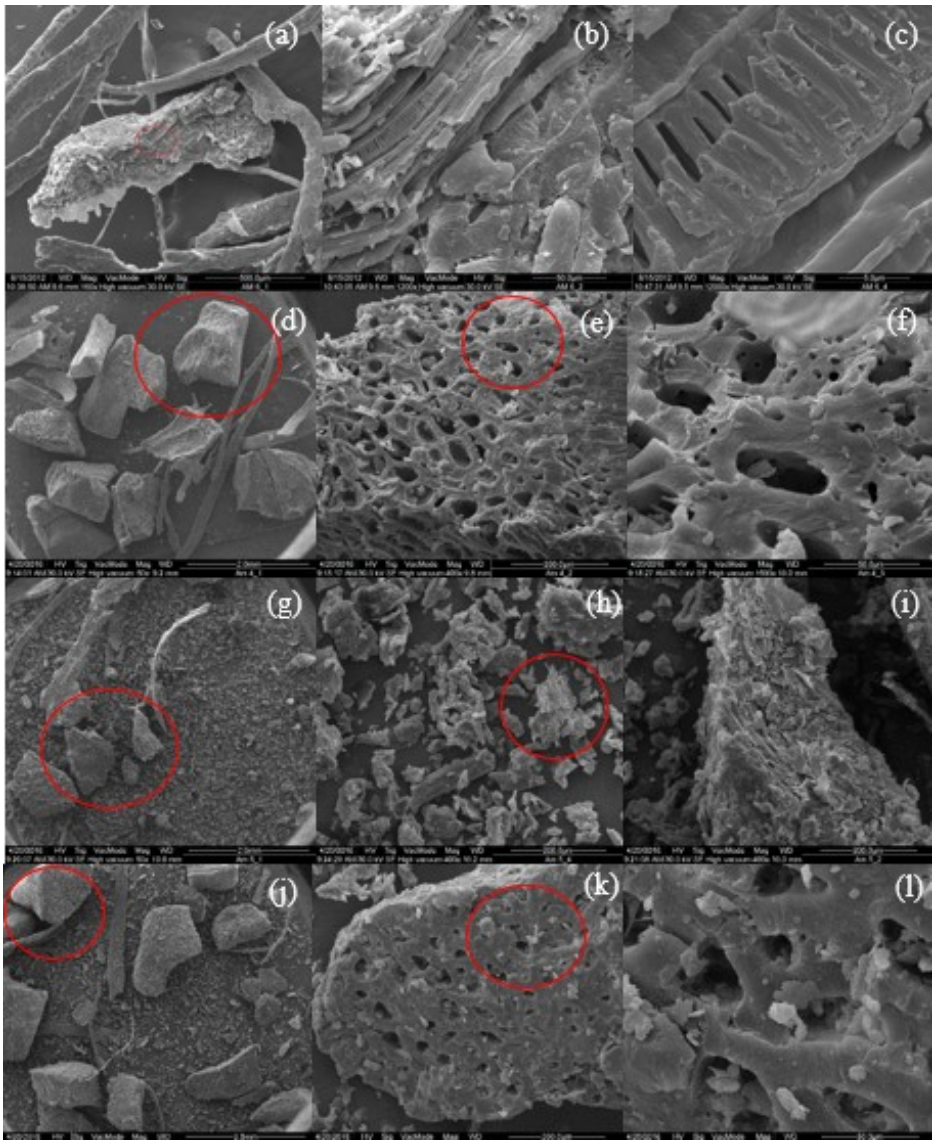

Figure 1. Scanning electron microscopy for fresh *E. Oleracea* (CA) endocarp under magnification of 160 (a) 1200 (b) and 12000 (c) times, and chemically modified with H_2O_2 under magnification of 50 (d), 400 (e), 1600 (f) times, modified with H_2SO_4 under magnification of 50 (g), 400 (h), 400 (i) times, and modified with NaOH under magnification of 50 (j), 400 (k) and 1600 (l) times.

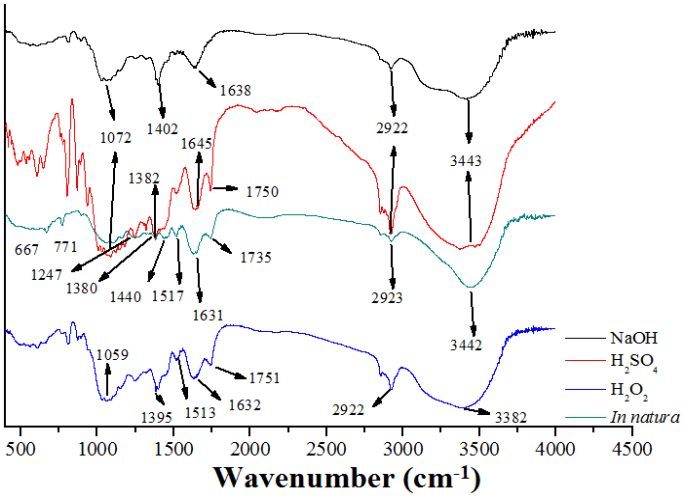

Figure 2. Infrared spectra of fresh CA and CA chemically modified with H_2O_2, H_2SO_4 and NaOH.

The region of 1750 and 1751 cm^{-1} in modification with H_2O_2 and H_2SO_4, and stretch of 1632, 1645 and 1638 cm^{-1} for H_2O_2, H_2SO_4 and NaOH, may be related to the C=O bonds of aldehydes, ketones, carbonyls,

amides and esters, respectively (Smidt & Meissl, 2007; Pavia et al., 2010). The stretch 1513 cm^{-1} for the modification with H_2O_2 refers to the presence of the aromatic skeleton of lignin (Smidt & Meissl, 2007).

The spectra in the regions 1395, 1382 and 1402 cm^{-1} for CA H_2O_2, H_2SO_4 and NaOH may be related to N-H bonds of amines (Smidt & Meissl, 2007; Pavia et al., 2010). The stretches in the region 1059 cm^{-1} for CA H_2O_2 and 1072 cm^{-1} for CA H_2SO_4 and NaOH, may be related to sulfoxides of S=O, C-OH bonds of oligosaccharides (Smidt & Meissl, 2007; Movasaghi, Rehman, & Rehman, 2008).

The adsorption of metal ions is related to the presence of functional groups, such as lignin, alcohols, carboxylic groups, proteins and carbohydrates. Various functional groups of fresh CA remained after the treatment with the modifying solutions indicating the presence of cellulose and lignin, which provide active sites for the adsorption process (Figure 2). However, other groups were also detected, such as sulfoxides and oligosaccharides, and thus alterations in the surface of the adsorbent have occurred in function of the modifying agents NaOH, H_2SO_4 and H_2O_2.

In general, the infrared spectra evidenced that the fresh CA and modified have in its surface, functional groups such hydroxyl, aliphatic, phenolic, carboxylic, which are the most likely to interact with the Cd, Pb and Cr in solution by physical interactions.

Point of zero charge (pH_{PZC})

Studies developed by Gonçalves Jr. et al. (2016) reported that the pH_{PZC} of fresh CA is 5.09. However, according to Figure 3, the results obtained by pH_{PZC} tests after treatment with the modifying solutions indicated that the point of zero charge for CA H_2O_2, H_2SO_4 and NaOH, changed to 4.41, 4.02 and 7.10, respectively. These changes were expected since the variation in pH_{PZC} occurred according to acidification or alkalinization power of each modifying solution, resulting in protonation, deprotonation or hydroxylation of chemical groups of CA.

When the pH > pH_{PZC}, the surface of the adsorbent is predominantly electronegative, favoring the adsorption of metal cations, such as Cd^{2+}, Pb^{2+} and Cr^{3+}. If the pH < pH_{PZC}, the adsorbent surface is predominantly electropositive, in which H^+ ions effectively compete with metal cations repelling them from the surface, and reducing the efficiency of adsorption.

In the studies conducted by Ribeiro et al. (2017), the authors observed that at higher pH dye adsorption was reduced, and at lower pH values, higher protonation occurred on the adsorbent surfaces, and that this favored the removal of the anion in solution (dye). Khandaker, Toyohara, Kamida, and Kuba (2018), who produced O_2-oxidized bamboo activated carbon, found that the pH_{PZC} of the activated carbon was 9.80, the authors state that this result suggests that the adsorbent surface is characterized by positive charges at pH's below of pH_{PZC}.

Thermogravimetric analysis

The thermogravimetric analyses were performed to verify the dynamics of weight loss and thermal stability after the treatment with H_2O_2, H_2SO_4 and NaOH. The TG and DTG curves are illustrated in Figure 4 for CA adsorbents modified with H_2O_2 (Figure 4a), H_2SO_4 (Figure 4b) and NaOH (Figure 4c). The first loss of mass is related to the release of moisture absorbed by the adsorbents, as well as the adsorption of water delimited by the surface tension began at lower temperature for CA H_2O_2 (66.81 to 100°C), CA H_2SO_4 (73.63 to 110ºC) and CA NaOH (72.42 to 100ºC). This fact can be explained by the oxidizing power of this modifying agent.

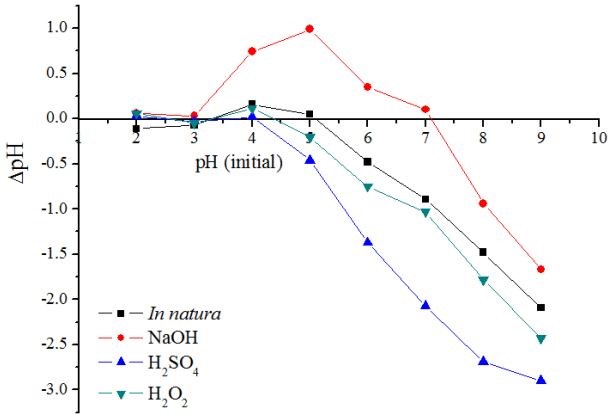

Figure 3. Point of zero charge (pH_{PZC}) of fresh CA and CA modified with H_2O_2, H_2SO_4 and NaOH.

The DTG curve related to decomposition of hemicellulose starts from 250, 250 and 230°C, for CA H_2O_2, CA H_2SO_4 and CA NaOH, respectively. However, the main cellulose loss for CA H_2O_2, CA H_2SO_4 occurred at 318.44 and 302.55°C, while for CA NaOH this step occurs at a lower temperature (287.90ºC). The decomposition of the lignin matrix and other compounds occurs above 392.50°C for CA H_2O_2 and CA H_2SO_4, and above 324.26°C for CA NaOH. The total loss of mass for CA H_2O_2 was 75 and 80% for CA H_2SO_4 and CA NaOH (Melzer, Blin, Bensakhria, Valette, & Broust, 2013; Moreira, Orsini, Vaz, Penteado, & Spinacé, 2016).

BET isotherms

The adsorption and desorption isotherms of BET for CA modified with NaOH, H_2SO_4 and H_2O_2, which are used for determining the specific surface area of the modified adsorbents as well as pore volume and diameter are presented in Figure 5.

It is possible to identify Type II BET isotherms, characteristic of non-porous or slightly porous systems. The modified adsorbents indicate an adsorption with negative concavity, representing the formation of monolayer. In this step high amounts of energy (Figure 5) are needed. A second convex segment refers to multilayer adsorption, involving low energy levels (Conradi Jr. et al., 2019). The parameters of specific surface area, pore volume and pore diameter are listed in Table 2.

According to Table 2, the specific surface area of adsorbents followed the sequence CA H_2O_2 > CA NaOH > CA H_2SO_4, and its values were, 0.5336, 0.1511 and 0.1396 $m^2\ g^{-1}$, respectively, The pore volume in $cm^3\ g^{-1}$ observed was 5.268 e^{-4}, 5.074 e^{-4} and, 3.330 e^{-4} for the sequence CA NaOH > CA H_2SO_4 > CA H_2O_2. The pore diameter was larger for CA NaOH (3.920 nm) > CA H_2O_2 (3.909 nm) > CA H_2SO_4 (3.291 nm). These results demonstrate that adsorption can occurs predominantly superficially, and it is low the possibility for intraparticle diffusion.

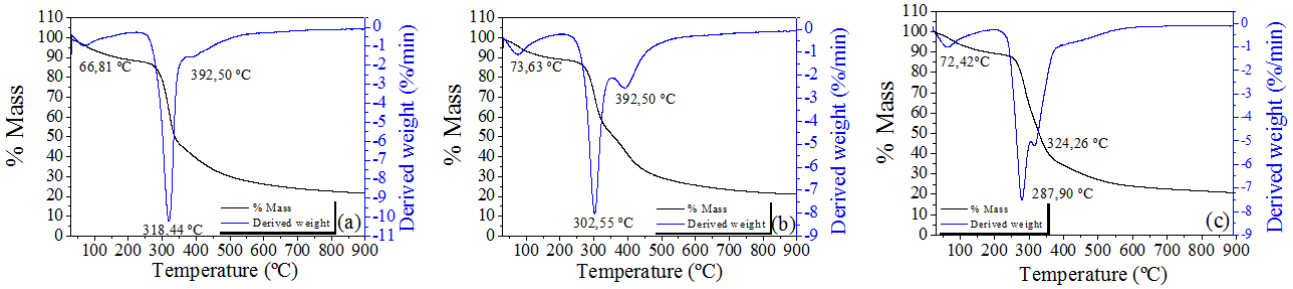

Figure 4. Thermogravimetric Analysis (TG) and Thermogravimetric Derivative (DTG) of CA chemically modified with H_2O_2 (a), H_2SO_4 (b) and NaOH (c).

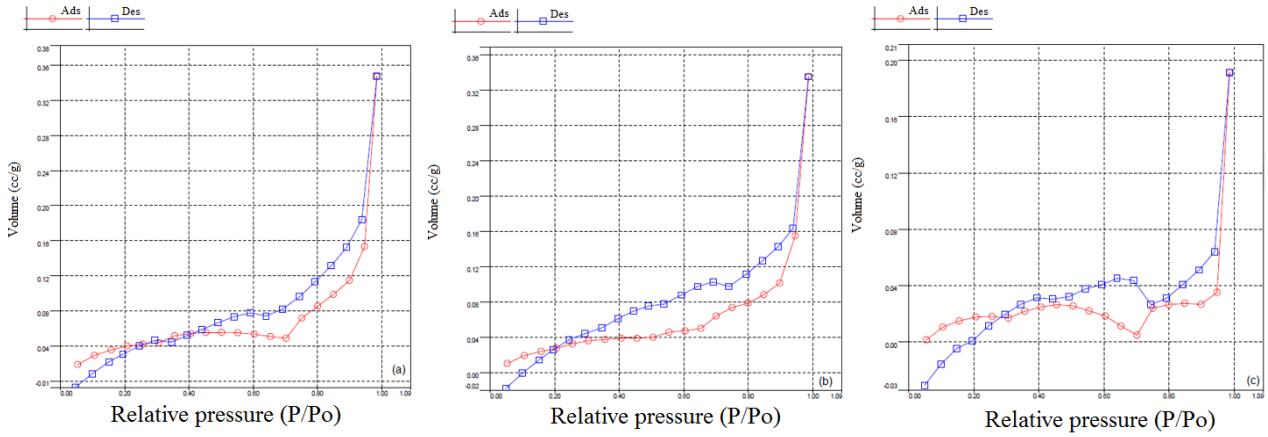

Figure 5. Adsorption and desorption isotherms of BET for CA chemically modified with NaOH (a), H_2SO_4 (b) and H_2O_2 (c).

Table 2. Surface area, volume and diameter of pores of CA chemically modified with NaOH, H_2SO_4 and H_2O_2.

Parameters	CA H_2O_2	CA H_2SO_4	CA NaOH
Surface area (SSA) ($m^2\ g^{-1}$)	0.5336	0.1396	0.1511
Pore volume ($cm^3\ g^{-1}$)	$3.330e^{-4}$	$5.074e^{-4}$	$5.268\ e^{-4}$
Pore diameter (nm)	3.909	3.291	3.920

It is observed that the surface area found for adsorbents derived from fresh CA (0.53 $m^2\ g^{-1}$ for CA H_2O_2; 0.13 $m^2\ g^{-1}$ for CA H_2SO_4; and 0.15 $m^2\ g^{-1}$ for CA NaOH) are very similar to other adsorbents found in the literature, as found by Penha et al. (2016) 1.13 $m^2\ g^{-1}$ in rice husk and by Oliveira and Franca (2011) 0.46 $m^2\ g^{-1}$ in rice bran.

Thus, the results demonstrate that the CA adsorbents have characteristics similar to other adsorbents derived from distinct biomasses, which have already proved potential to remediate waters and other compartments. Thus the CA adsorbents may also be favorable to adsorption of metallic ions such as Cd, Pb and Cr.

Multivariate analysis for adsorbent dose and pH influence

The results of the multivariate analysis by CCD are listed in Table 3, whose results were evaluated by an ANOVA (Table 4 and 5).

According to Table 4, there was a significant difference at 5% of significance for all adsorbents among studied variables, except for Pb^{2+} and Cr^{3+} when adsorbed by fresh CA and CA H_2O_2. The same can observed in Pareto graphs (Figure 6e, i, j). In some isolated cases, there was significant difference in pH and dose, such as for ions Cd^{2+} for fresh CA (Figure 6a), CA H_2SO_4 (Figure 6c), and Cr^{3+} by CA NaOH (Figure 6j). In other cases, there was difference only for the adsorbent dose, such as Cd^{2+} by CA H_2O_2 (Figure 6b) and Pb^{2+} by CA H_2O_2 (Figure 6f) or only among the studied pH values, such as Cr^{3+} for CA H_2SO_4 (Figure 6k). These results demonstrate that the adsorption capacity of the fresh and modified materials depends in great part on the adsorbent dose, and in small part on the solution pH.

The response surfaces graphs for Cd^{2+}, Pb^{2+} and Cr^{3+} adsorption by fresh CA, CA H_2O_2, CA H_2SO_4 and CA NaOH shown in Figure 7 (a, b and c) are also expressed by the equations exhibited in Table 5. According to the obtained results, the higher Q_{eq} were obtained with reduced availability of adsorbent material in solution, i.e., 200 mg of fresh and chemically modified adsorbents, i.e., 4 g L^{-1} are required for obtaining the highest adsorption efficiency.

Table 3. CCD matrix with triplicate in the central point, coded values and real mean values for the adsorption of Cd^{2+}, Pb^{2+} and Cr^{3+} for fresh adsorbent and modified with H_2O_2, H_2SO_4 and NaOH.

Test	Variables		Q_{ads} (mg g^{-1}) Cd^{2+}				Q_{ads} (mg g^{-1}) Pb^{2+}				Q_{ads} (mg g^{-1}) Cr^{3+}			
	Mass (mg)	pH	Fresh CA	CA H_2O_2	CA H_2SO_4	CA NaOH	Fresh CA	CA H_2O_2	CA H_2SO_4	CA NaOH	Fresh CA	CA H_2O_2	CA H_2SO_4	CA NaOH
1	396.39	3.6	1.035	0.866	0.164	1.240	0.938	1.163	0.807	1.077	0.725	0.820	0.427	1.131
2	1103.61	3.6	0.408	0.396	0.066	0.435	0.334	0.437	0.294	0.351	0.313	0.343	0.165	0.417
3	396.39	6.4	0.663	1.077	0.347	1.157	0685	1.225	1.025	1.065	0.771	1.162	0.805	0.659
4	1103.61	6.4	0.421	0.427	0.062	0.436	0.252	0.442	0.342	0.370	0.259	0.360	0.245	0.187
5	750.00	5.0	0.617	0.612	0.140	0.650	0.498	0.644	0.450	0.538	0.465	0.471	0.096	0.494
6	250.00	5.0	1.612	1.596	0.687	1.981	1.673	1.855	1.332	1.744	1.202	0.889	0.322	1.792
7	750.00	7.0	0.616	0.631	0.148	0.652	0.465	0.627	0.554	0.557	0.560	0.511	0.597	0.395
8	1250.00	5.0	0.367	0.379	0.056	0.386	0.279	0.386	0.261	0.310	0.325	0.316	0.058	0.243
9	750.00	3.0	0.502	0.391	0.070	0.659	0.465	0.458	0.239	0.556	0.072	0.000	0.000	0.637
10	750.00	5.0	0.610	0.622	0.143	0.651	0.480	0.640	0.429	0.542	0.506	0.457	0.047	0.506
11	750.00.	5.0	0.616	0.593	0.152	0.653	0.505	0.646	0.425	0.538	0.487	0.467	0.052	0.520
12	750.00	5.0	0.590	0.595	0.121	0.650	0.486	0.641	0.428	0.525	0.493	0.483	0.042	0.505

Q_{ads}: Adsorbed amount of metal ions in mg g^{-1}. Experimental conditions: volume: 50 mL concentration of Cd^{2+}, Pb^{2+} and Cr^{3+} (10 mg L^{-1}), stirring time: 90 min., stirring rpm: 200; temperature: 25°C.

Table 4. Analysis of variance (ANOVA) of the model predicted for the influence of the adsorbent mass of fresh *Euterpe Oleracea* endocarp (CA), CA H_2O_2, CA H_2SO_4 and CA NaOH, and pH influence in the removal of Cd^{2+}, Pb^{2+} and Cr^{3+}.

SV	DF	Cd^{2+}				Pb^{2+}				Cr^{3+}			
		Fresh CA	CA H_2O_2	CA H_2SO_4	CA NaOH	Fresh CA	CA H_2O_2	CA H_2SO_4	CA NaOH	Fresh CA	CA H_2O_2	CA H_2SO_4	CA NaOH
Mass (L)	1	1.04*	1.00*	294.35*	1.872	1.781	1.608*	0.056	0.0513*	11.48	2.903	0.114	3.824*
Mass (Q)	1	0.24*	0.19*	11.27	0.387	1.213	0.352*	0.452	0.139	9.91	0.426	3.651	0.187
pH (L)	1	0.02*	0.042	691.38*	$1.81e^{-6}$	1.781	0.011	11.28*	2.14	1.66	23.87	38.34*	24.59*
pH (Q)	1	0.003^{ns}	0.024	279.36*	0.002	1.213	0.018	0.021	2.062*	0.05	5.341	31.911*	0.016
Mass x pH	1	0.009^{ns}	0.008	24.39	$3.9\ e^{-6}$	0.010	0.001	0.118	0.035*	0.44	1.238	0.338	0.369
Residual	6	0.002	0.009	20.189	0.0107	0.717	0.007	0.576	0.346	2.79	4.385	2.336	0.452
Total	11												

*Significant at 5% probability by F-test (Barros et al., 2010). ^{ns}Non-significant at 5% by F-test. SV: Sources of variation. DF: Degrees of freedom.

Table 5. Equations for the response surface analysis of the adsorbed amount (Q_{ads}) of Cd^{2+}, Pb^{2+} and Cr^{3+} by CA fresh and modified with H_2O_2, H_2SO_4 and NaOH in tests of adsorbent mass and pH.

CA	Q_{ads}	R^2
	Cd^{2+}	
fresh:	$2,069 + 0.1355x - 0.0298x^2 - 0.0037y + 0.0000012y^2 + 0.00019xy$	0.864
H_2O_2	$0.7820 + 0.4280x - 0.0308x^2 - 0.0026y + 0.0000014y^2 - 0.0000911xy$	0.961
H_2SO_4	$0.0085 + 0.2704x - 0.1739^2 - 0.0011y + 0.00000076y^2 - 0.000094xy$	0.865
NaOH	$2.649 + 0.0743x - 0.01143x^2 - 0.0443y + 0.0000019y^2 + 0.0000424xy$	0.961
	Pb^{2+}	
fresh	$5,753 - 1,7633x + 0,2173x^2 + 0,00040y + 0,0000005y^2 - 0,00010xy$	0.448
H_2O_2	$1,7314 + 0,3188x - 0,0270x^2 - 0,00394y + 0,0000018y^2 - 0,000028xy$	0.978
H_2SO_4	$8.3212 - 1.3848x + 0.02872x^2 + 0.00169y - 0.0000021y^2 + 0.000343xy$	0.776
NaOH	$-1.59516 + 0.8204x - 0.0613x2 + 0.00322y - 0.0000006y2 - 0.00029xy$	0.695
	Cr^{3+}	
fresh	$26.3232 - 7.5633x + 0.6218x^2 - 0.0057y + 0.00000075y^2 + 0.00066xy$	0.579
H_2O_2	$24.71843 - 6.61449x + 0.45616x^2 - 0.00414y - 0.00000204y^2 + 0.00110xy$	0.569
H_2SO_4	$-12.5686 + 9.15875x - 1.1141x^2 + 0.00665y - 0.0000061y^2 + 0.00057xy$	0.836
NaOH	$-1.4854 + 0.50977x + 0.0256x^2 - 0.003y + 0.0000013y^2 + 0.000628xy$	0.914

CA: *açaí* endocarp; Q_{ads}: amount adsorbed (mg g^{-1}); R^2: coefficient of determination.

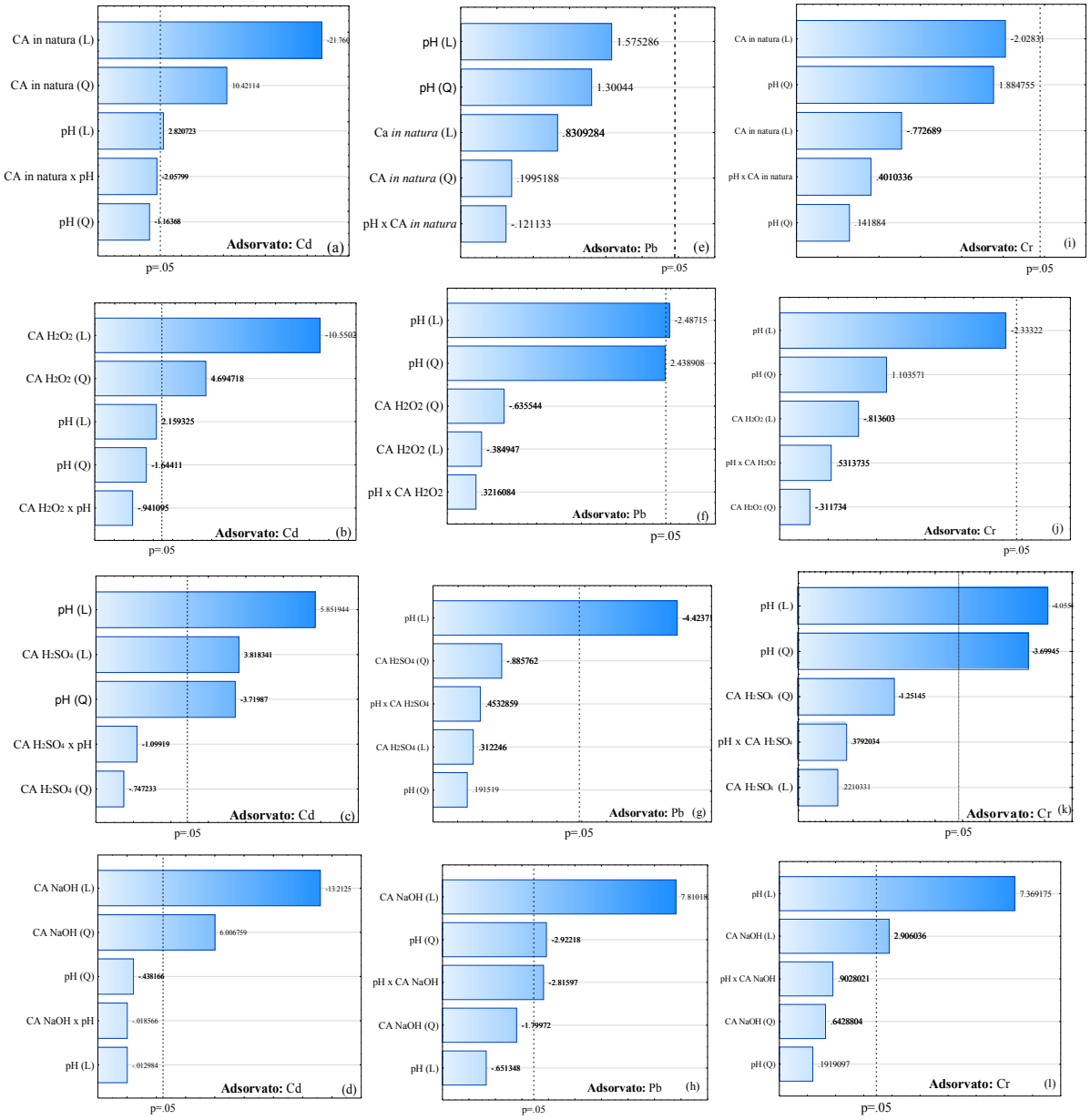

Figure 6. Pareto chart obtained in CCD for multivariate analysis for adsorbent mass (dose) and pH on the sorption of Cd^{2+} (a, b, c, d), Pb^{2+} (e, f, g, h) and Cr^{3+} (i, j, k, l) on the *açaí* endocarp (CA) fresh and modified with H_2O_2, H_2SO_4 and NaOH.

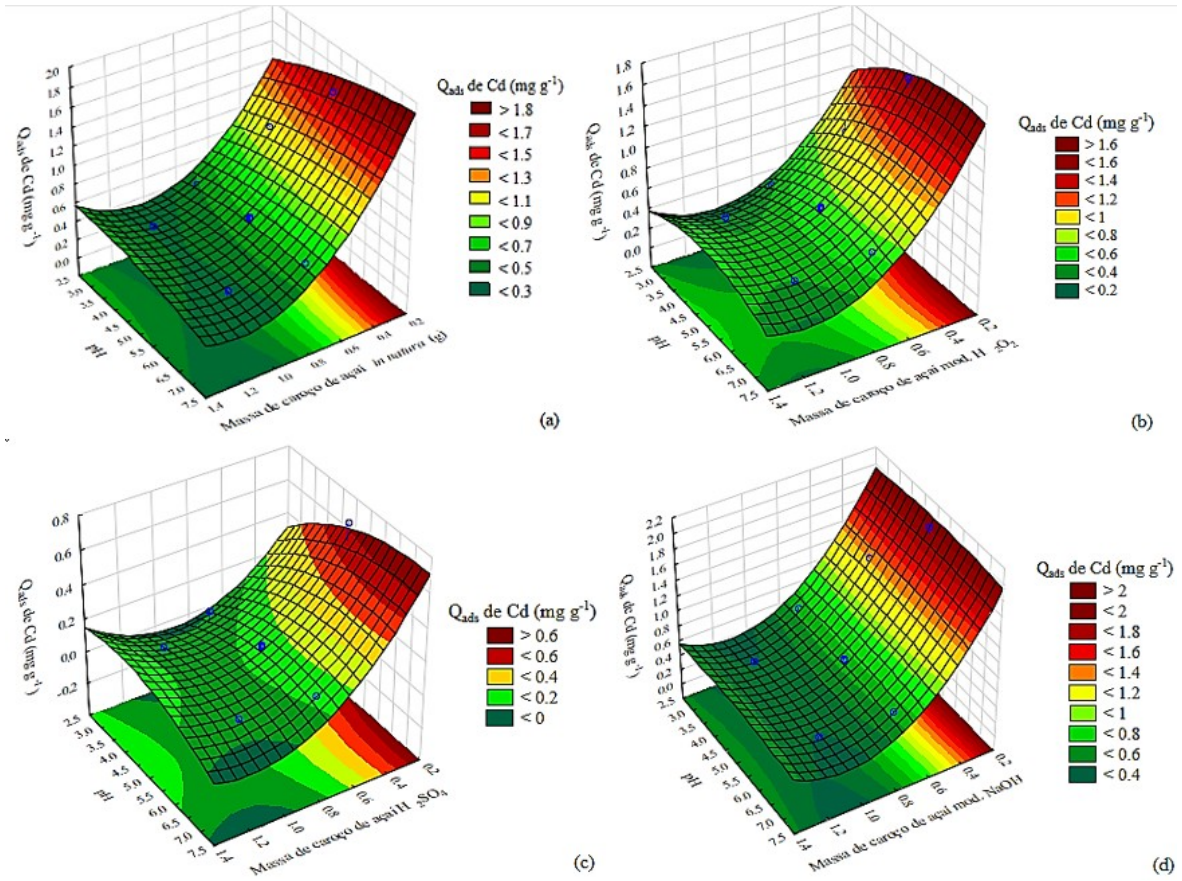

Figure 7A. Response surface graph for multivariate analysis for adsorbent dose and pH of the solution according to the adsorbed amount (Q_{ads}) of Cd^{2+} (a, b, c, d) on the *açaí* endocarp (CA) fresh (a) and modified with H_2O_2 (b), H_2SO_4 (c) and NaOH (d).

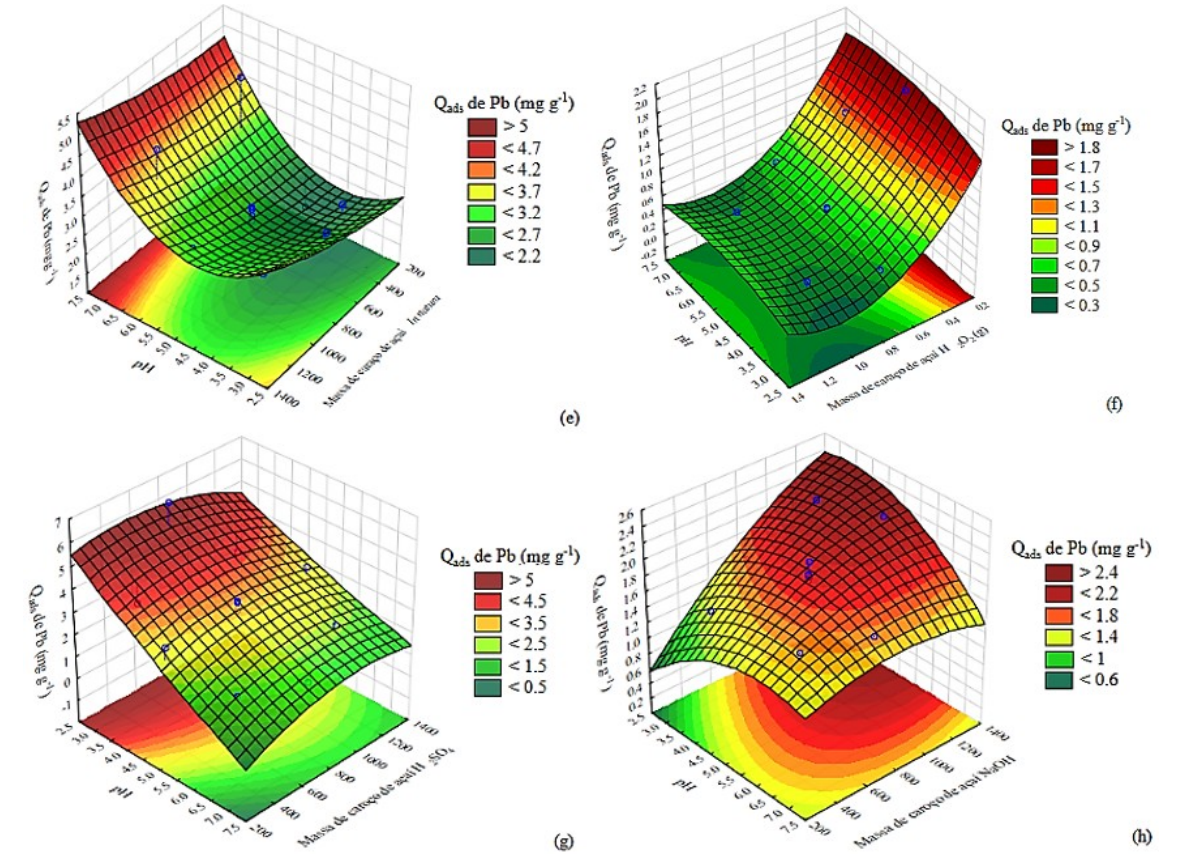

Figure 7B. Response surface graph for multivariate analysis for adsorbent dose and pH of the solution according to the adsorbed amount (Q_{ads}) of Pb^{2+} (e, f, g, h) on the *açaí* endocarp (CA) fresh (a) and modified with H_2O_2 (b), H_2SO_4 (c) and NaOH (d).

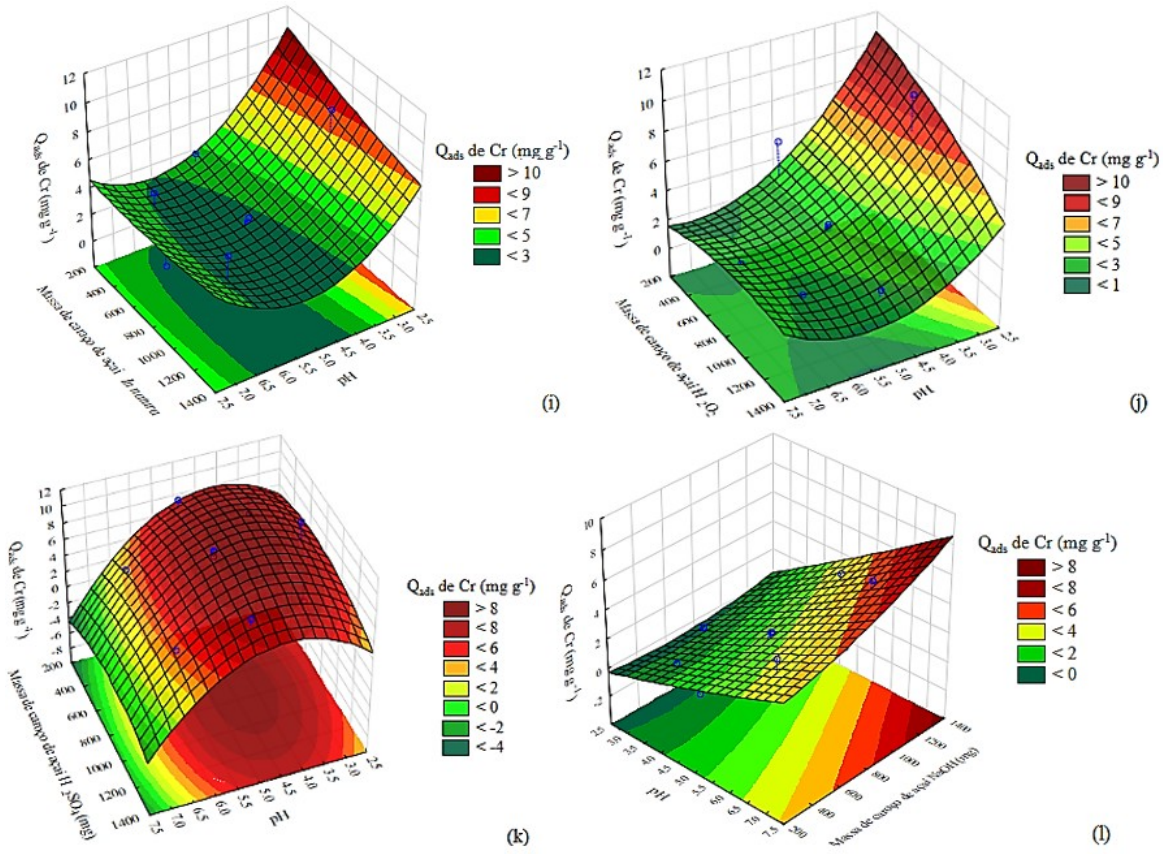

Figure 7C. Response surface graph for multivariate analysis for adsorbent dose and pH of the solution according to the adsorbed amount (Q_{ads}) of Cr^{3+} (i, j, k, l) on the *açaí* endocarp (CA) fresh (a) and modified with H_2O_2 (b), H_2SO_4 (c) and NaOH (d).

Even in certain cases, there may be a decrease in the amount adsorbed due to formation of agglomerates, which will reduce the total surface area and thus the number of active sites available for the adsorption process (Rubio et al., 2013a; 2013b; Kiran, Srikantaswamy, Pallavi, Manoj, & Tasneem, 2013; Coelho et al., 2014).

Nacke et al. (2016) and Gonçalves Jr. et al. (2016) investigated the influence of the dose of fresh *Jatropha curcas* L. and fresh CA in the removal of Cu^{2+} and Zn^{2+}, and found that 8 g L^{-1} was enough for removing these metal ions in contaminated solution. Schwantes et al. (2015; 2016) performed chemical changes in crambe meal and cassava peels with H_2O_2, H_2SO_4 and NaOH and obtained 200 mg per 50 mL (4 g L^{-1}) as the optimum amount for removal of Cd^{2+}, Pb^{2+} and Cr^{3+} at pH 5.0.

Ercan and Aydin (2013) recommend that adsorption tests should be conducted at a maximum pH of 5.0. According to these authors, at pH above of 6.0, precipitation of ions Cd^{2+}, Pb^{2+} and Cr^{3+} may occurs, making them unavailable for adsorption. Conradi Jr. et al. (2019) reported that Pb is present in free form (Pb^{2+}) until pH 6.0. In alkaline conditions above 6.0, hydroxyl species can be formed and they are insoluble, influencing the results by causing a decrease in the adsorbed amount. In this way, for adsorption testing purposes, pH 5.0 was considered as the best for the removal process. This value tends to favor the CA H_2O_2 and CA H_2SO_4 adsorbents, because pH is above pH_{PZC} (Figure 3) of these materials, increasing the proportion of superficial negative charges that favors for the adsorption of cations.

Influence of the contact time

The effect of the contact time of Cd^{2+}, Pb^{2+} and Cr^{3+} on CA H_2O_2, CA H_2SO_4 and CA NaOH adsorbents is exhibited in Figure 8. The results evidence that the sorption of toxic metals by *Euterpe Oleracea* based adsorbents is a fast process, occurring in the first moments and with a slight decrease over time. In approximately 40 min. the process reaches the equilibrium. After that, the active sites of the adsorbent are depleted, and Q_{ads} of Cd^{2+}, Pb^{2+} and Cr^{3+} started to be controlled by the transport rate from the outside to the inside of the active sites of the particles of adsorbents (Nacke et al., 2017). This also mean that periods of contact time longer than 40 min. can be ineffective in the removal of metals on a large scale. Only Cr^{3+} achieved a reduction of Q_{ads} on CA NaOH after equilibrium time.

Assessment of the adsorption kinetic mechanism

The adsorption kinetics for Cd^{2+}, Pb^{2+} and Cr^{3+} in the adsorbents modified with H_2O_2, H_2SO_4 and NaOH was evaluated by the pseudo-first order, pseudo-second order, Elovich and intraparticle diffusion models (Table 6 and Figure 9).

According to Table 6, the pseudo-first order, Elovich and intraparticle diffusion models did not achieve good fitting to the experimental data, with values of $Q_{eq(exp.)}$ and $Q_{eq(calc.)}$ far from each other. Gonçalves Jr. et al. (2016), Nacke et al. (2016) and Coelho et al. (2014) investigated the adsorption kinetics of fresh CA, *Jatropha curcas* and cashew nut shell, and found the best adjustments for pseudo-second-order model for Cu^{2+}, Zn^{2+}, Cd^{2+}, Pb^{2+} and Cr^{3+}, respectively. The similar situation was observed for chemically modified adsorbents of crambe meal and cassava peel studied by Schwantes et al. (2015) and Schwantes et al. (2016).

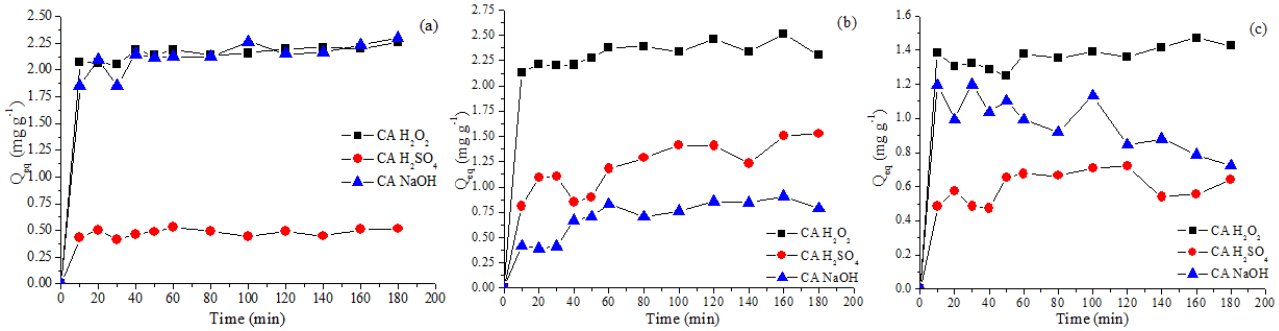

Figure 8. Effect of the contact time of CA modified with H_2O_2, H_2SO_4 and NaOH in the removal of metal ions Cd^{2+} (a), Pb^{2+} (b), Cr^{3+} (c).

Table 6. Kinetic parameters obtained for the study of Cd^{2+}, Pb^{2+} and Cr^{3+} adsorption on CA by means of pseudo-first order, pseudo-second order, Elovich, intraparticle diffusion.

Adsorbents		Pseudo-first order			Pseudo-second order			Elovich		
		K_1 (min.$^{-1}$)	$Q_{eq\ (cal.)}$ (mg g^{-1})	R^2	K_2 (g mg^{-1} min.$^{-1}$)	$Q_{eq\ (cal.)}$ (mg g^{-1})	R^2	A (mg g^{-1} hour^{-1})	B (g mg^{-1})	R^2
Cd	Fresh	-0.017	0.159	0.948	0.488	1.170	0.999	-22.438	23.605	0.957
	H_2O_2	-0.0980	0.2278	0.921	0.2002	2.2478	0.999	1.7315	0.0965	0.904
	H_2SO_4	-0.0107	0.1276	0.755	0.7100	0.5006	0.986	0.2966	0.0375	0.388
	NaOH	-0.0106	0.4473	0.800	0.1045	2.2937	0.997	1.5587	0.1383	0.910
Pb	Fresh	-0.011	0.076	0.876	0.692	0.491	0.998	-17.155	45.683	0.933
	H_2O_2	-0.2746	1.0610	0.821	635.6701	0.1019	0.959	1.7310	0.1490	0.876
	H_2SO_4	-0.3116	0.8959	0.867	85.5662	0.0616	0.926	0.3163	0.2303	0.951
	NaOH	-0.2347	0.5924	0.879	-5.9363	0.1549	0.966	-0.1311	0.1995	0.842
Cr	Fresh	-0.012	0.157	0.622	0.926	0.493	0.994	-3.175	15.475	0.927
	H_2O_2	-0.0079	0.1847	0.912	0.1525	1.5198	0.997	1.0869	0.0663	0.647
	H_2SO_4	-0.0341	0.4974	0.793	28.2170	0.6001	0.943	0.2091	0.1064	0.792
	NaOH	0.0069	0.1377	0.908	-0.1063	0.7446	0.969	1.6974	-0.1702	0.840

		Intraparticle diffusion									
		K_{id} (g mg^{-1} min.$^{-1/2}$)			C_i (mg g^{-1})			R^2			$Q_{eq(exp.)}$ (mg g^{-1})
		Line A	Line B	Line C	Line A	Line B	Line C	Line A	Line B	Line C	
Cd	Fresh	-20.657	-111.524	-	22.460	105.952	-	0.865	0.984	-	1.120
	H_2O_2	0.0281	-0.013	0.0206	1.9587	2.2805	1.9656	0.075	-0.174	0.455	2.2571
	H_2SO_4	0.0548	0.0467	0.0234	0.2607	0.1649	0.1979	-	0.941	0.665	0.5305
	NaOH	0.0889	0.0468	0.0624	1.6208	1.7620	1.4527	0.604	0.542	0.876	2.3031
Pb	Fresh	-36.000	-40.719	-	92.815	109.299	-	0.789	0.689	-	0.459
	H_2O_2	0.029	0.056	0.063	2.049	1.903	1.729	0.721	0.417	0.727	2.3128
	H_2SO_4	0.427	0.397	0.863	0.132	0.101	0.05	0.655	0.985	0.977	1.1929
	NaOH	-0.001	0.012	0.047	0.417	0.606	0.305	-0.934	0.155	0.766	0.6916
Cr	Fresh	-8.715	68.145	-	34.005	-118.463	-	0.960	0.784	-	0.450
	H_2O_2	-0.024	-0.003	0.023	1.433	1.408	1.122	0.488	-0.777	0.401	1.4733
	H_2SO_4	-0.003	0.016	0.063	0.496	0.542	-0.213	-0.844	0.755	0.694	0.5974
	NaOH	-0.032	-0.056	-0.055	1.307	1.435	1.480	0.200	0.460	0.596	0.7250

K_1: pseudo-first-order rate constant; Q_{eq}: amount of adsorbate retained per gram of adsorbent at equilibrium; K_2: pseudo-second order rate constant; A: constant indicating the initial chemisorption rate; B: number of sites suitable for adsorption, related to the surface cover extension and the activation energy of chemisorption; R^2: coefficient of determination; K_{id}: intraparticle diffusion constant; C_i: suggests the thickness of the boundary layer effect.

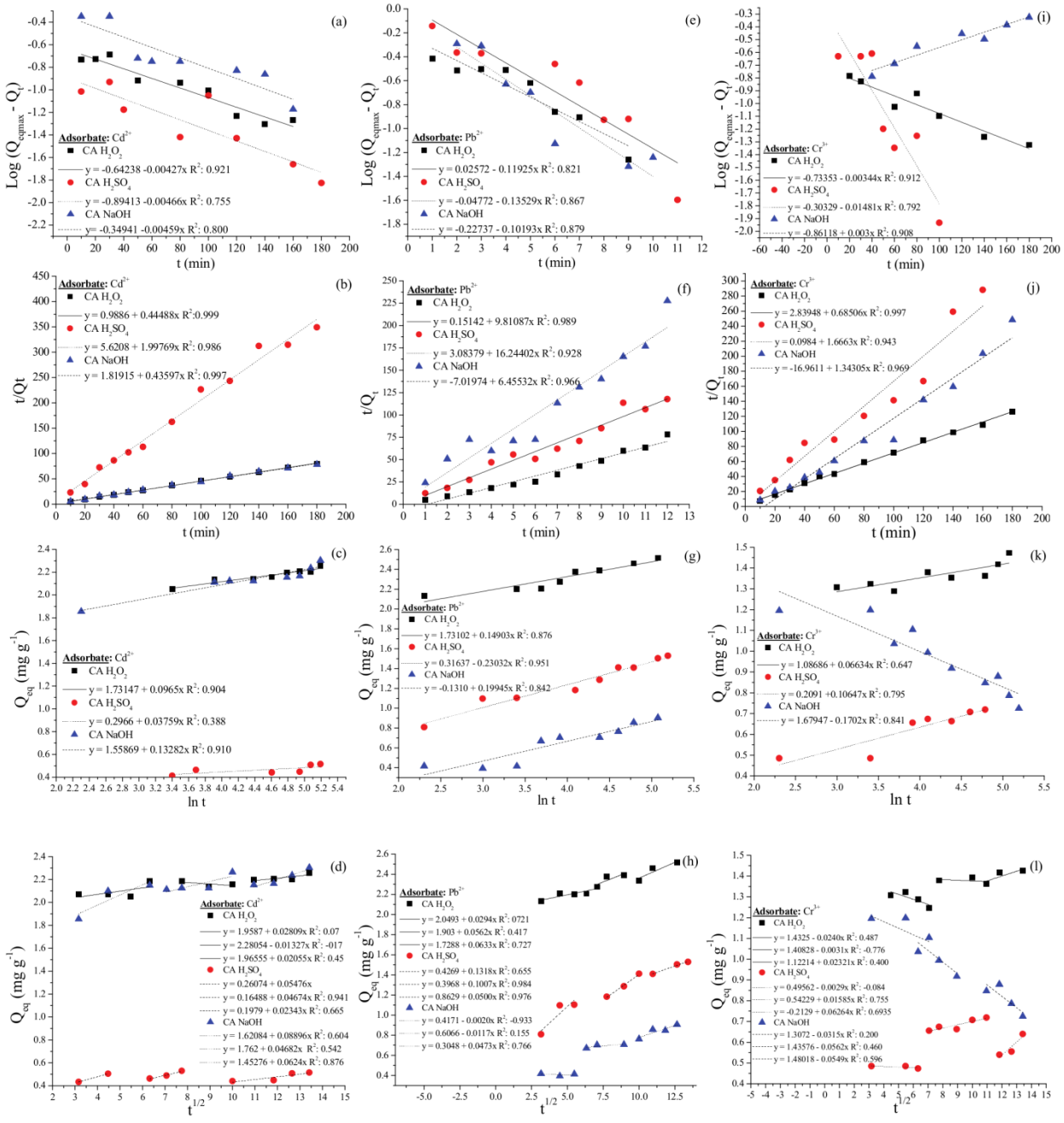

Figure 9. Kinetic models of pseudo-first order (a, e, i), pseudo-second order (b, f, j), Elovich (c, g, k) and intraparticle diffusion (d, h, l) for sorption of Cd^{2+}, Pb^{2+} and Cr^{3+} respectively, for CA modified with H_2O_2, H_2SO_4 and NaOH.

In this research, by performing chemical changes, the pseudo-second order model showed better adjustments for adsorption of Cd^{2+} and Cr^{3+} by *Euterpe Oleracea* based adsorbents. Also, the $Q_{eq(exp.)}$ and $Q_{eq(calc.)}$ values for *Euterpe Oleracea* modified adsorbents are closer. However, for Pb^{2+} the same dynamic was not verified. Thus, it is suggested that the adsorption kinetics of Cd^{2+} and Cr^{3+} follows the pseudo-second order model, which, according to Conradi Jr. et al. (2019), in these cases the chemisorption may be a limiting factor of the process because will involve the sharing of electrons among metals and the modified adsorbents.

Adsorption and desorption efficiency, and the possibility of reusing the CA adsorbents

From the isotherms studies, it was possible to evaluate the efficiency of adsorption (%) and desorption (%) of Cd^{2+}, Pb^{2+} and Cr^{3+} on fresh CA, CA H_2O_2, CA H_2SO_4 and CA NaOH (Figure 10).

The dynamic of the removal of toxic metals was influenced by its initial concentration in solution. According to Figure 10, the adsorption efficiency, in general, decreases with the increasing initial concentration. In agreement with Bohli et al. (2015), this dynamic involves the metal ion/adsorbent ratio,

when this ratio is low, the adsorption occurs preferentially in higher energy sites. After that, the sites with higher energy become saturated as this ratio increases, and finally, the adsorption of the ions may occur involving sites with lower energy, thus resulting in the decrease of absorption efficiency.

In the case of Cd^{2+} for fresh CA, CA H_2O_2 and CA H_2SO_4, and in the case of Pb^{2+} for CA H_2O_2, the adsorption efficiency was 73.2, 74.7, 71.2 and 78.8%, respectively, in initial concentrations. The highest percentages of desorption were achieved for Cd^{2+} in fresh CA and for Pb^{2+} for fresh CA, CA H_2O_2 and CA H_2SO_4, with efficiency of 90.9, 92.9, 98.9 and 95.7%, respectively, in initial concentrations.

Cr^{3+} showed the lowest desorption rates by studied adsorbents (Figure 10i, j, k, l). Similar results were obtained by *Moringa oleifera* L. meal (Meneghel et al., 2013), meal of *Crambe abyssinica* H. (Rubio et al., 2013b), cashew nut shell (Coelho et al., 2014), fresh cassava peel (Schwantes et al., 2015).

According to these aforementioned authors, low desorption values are a strong indication that this metal is adsorbed by chemical bonds (chemisorption), which prevents its reuse in new sorption cycles. In general, modified adsorbents, when compared to fresh adsorbents, show higher adsorption efficiency, which is positive because it is a simple treatment, with low-cost, and can raise the adsorption capacity of adsorbents produced by agribusiness that also have high availability (Coelho et al., 2014; Schwantes et al., 2016).

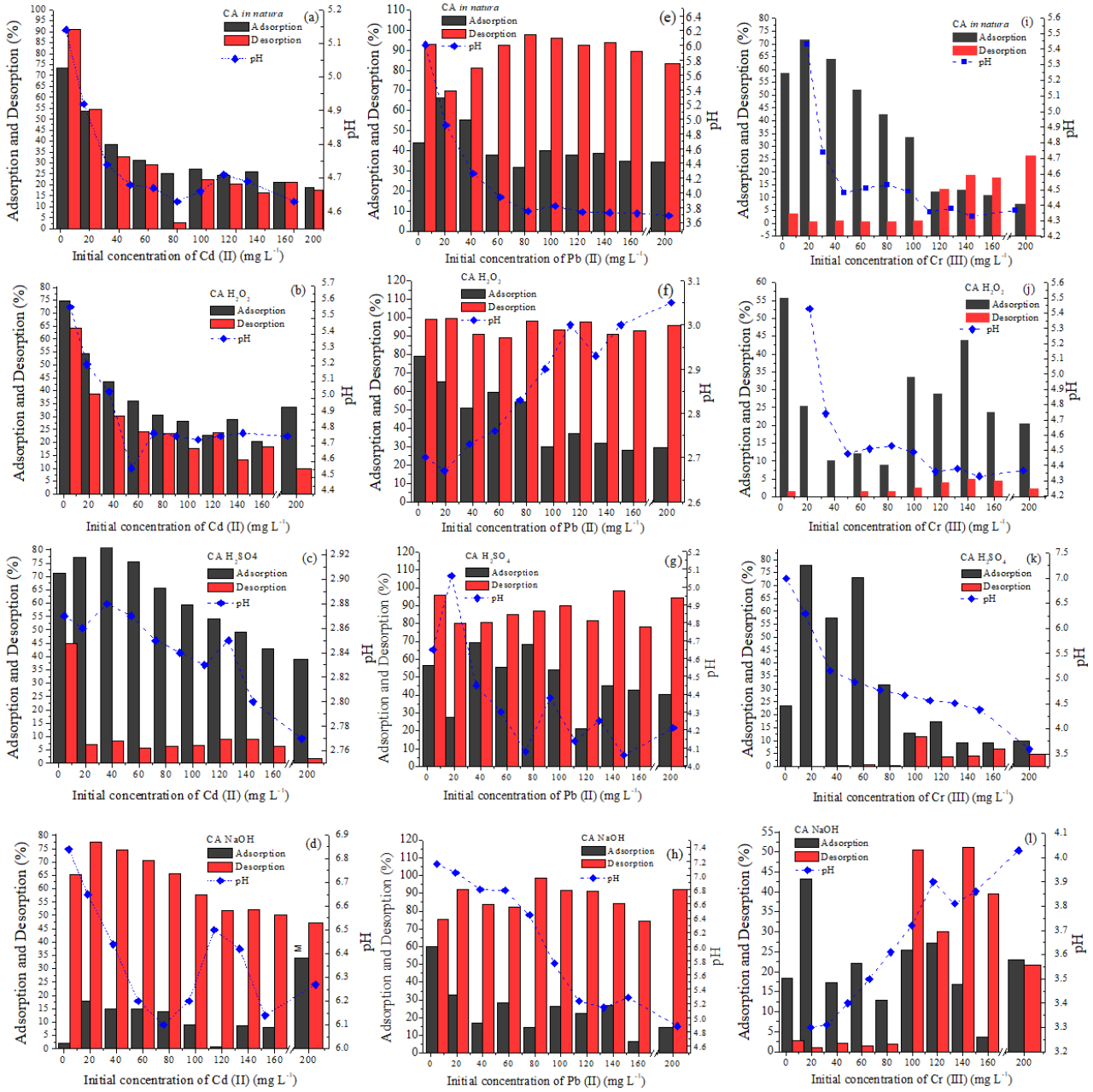

Figure 10. Adsorption (%), Desorption (%) and pH after adsorption of Cd^{2+} (a, b, c, d), Pb^{2+} (e, f, g, h) and Cr^{3+} (i, j, k, l), respectively, by CA fresh and modified with H_2O_2, H_2SO_4 and NaOH.

According to Figure 10, in most of the cases it was observed an acidification of the pH after adsorption of Cd^{2+}, Pb^{2+} and Cr^{+3}; also, the adsorbents modified with H_2SO_4 showed the highest acidification of the solution. Exception for the adsorption of Pb^{2+} on CA H_2O_2 and Cr^{3+} on CA NaOH, a slight solution alkalization was shown.

This first observation is usually related to ion exchange (physical) and the second, to chemisorption. Data showed that the mechanisms acting on the adsorption process are complex. The pH change can occur due to the interaction of ion exchange in the solution. The biosorbents surface have a negative charge because of the presence of organic functional groups, such as carboxylic or hydroxyl (Bartczak et al., 2018), which are able to participate in ion exchange as presented in Equation 8 and 9.

$$C{-}COOH + M^{n+} \leftrightarrow C{-}COOM + nH^{+} \quad (8)$$

$$C{-}COOH + M^{n+} \leftrightarrow C{-}COOM(OH) \quad (9)$$

It may also form hydrolyzed species (Equation 10):

$$M^{n+} + H_2O \leftrightarrow M(OH)^{n} + H^{+} \quad (10)$$

Adsorption isotherms

Adsorption isotherms can be classified into classes and subgroups as proposed by Giles, MacEwan, Nakhwa, and Smith (1960). Thus, the isotherms of metal ions Cd^{2+}, Pb^{2+} and Cr^{3+} by CA modified with H_2O_2, H_2SO_4 and NaOH (Figure 11) could be classified in the class '*L*' because their dynamics suggest the decrease of the availability of active sites with increased concentration (Giles et al., 1960).

The convex shape displayed by adsorption isotherms is favorable, showing a tendency to equilibrium by saturation of the adsorbent active sites, corroborating to the monolayer theory of Langmuir, which allows us to infer the maximum adsorption capacity (Conradi Jr. et al., 2019).

For Pb^{2+} and Cr^{3+} adsorbed by CA H_2SO_4 (Figure 10g and k), it is observed an isotherm specific of the subgroup 2 of class '*L*', indicating the saturation of the surface in which Cr^{3+} ions have a higher preference for the adsorbent surface than for the already adsorbed molecules (Giles et al., 1960).

The parameters of Langmuir and Freundlich (Table 7) were obtained by nonlinear models (Figure 11) and Dubinin-Radushkevich (D-R) (Table 8) by linear models of adsorption isotherms.

For adsorption of Cd^{2+}, Pb^{2+} and Cr^{3+} by CA fresh and chemically modified with H_2O_2, H_2SO_4 and NaOH, Langmuir and Freundlich adjustments proved to be satisfactory, as can be seen by R^2 values (Table 7).

According to Gonçalves Jr. et al. (2016), in this case, there are more than one type of adsorption site, resulting in the occurrence of adsorption in both mono and multilayer. The R_L of Langmuir considers favorable for adsorption the values greater than zero and minors than one (Sun, Sun, & Sun, 2013), as observed in this study (Table 7).

Table 7. Parameters of nonlinear mathematical models of Langmuir and Freundlich related to adsorption of Cd^{2+}, Pb^{2+} and Cr^{3+} on *Euterpe Oleracea* endocarp (CA) fresh and modified with H_2O_2, H_2SO_4 and NaOH.

Adsorbents	Langmuir Constants						Freundlich Constants				
	Q_m (mg g^{-1})	EP	*b or* K_L (L mg^{-1})	*SE*	R_L	R^2	K_f (mg g^{-1})	*EP*	*n*	*SE*	R^2
				Cd^{2+}							
Fresh	11.751	1.4365	0.0173	0.0051	0.224	0.939	0.847	0.1299	0.466	0.0336	0.979
H_2O_2	9.097	0.5035	0.0392	0.0066	0.113	0.978	1.173	0.1550	0.400	0.0308	0.979
H_2SO_4	3.414	0.2916	0.0967	0.0299	0.050	0.924	0.653	0.2042	0.362	0.0806	0.825
NaOH	31.714	3.7610	0.0097	0.0022	0.338	0.980	0.814	0.2302	0.637	0.0609	0.968
				Pb^{2+}							
Fresh	47.461	24.0577	0.0041	0.0029	0.549	0.919	0.483	0.2083	0.727	0.0957	0.933
H_2O_2	15.011	1.5228	0.0431	0.0149	0.104	0.904	2.057	0.6771	0.385	0.0747	0.866
H_2SO_4	81.197	94.451	0.0017	0.0022	0.716	0.977	0.162	0.0509	0.935	0.0768	0.977
NaOH	33.533	4.8618	0.0083	0.0023	0.375	0.970	0.805	0.3063	0.629	0.0800	0.943
				Cr^{3+}							
Fresh	10.235	0.7601	0.0950	0.0243	0.050	0.963	1.863	0.68295	0.386	0.1002	0.834
H_2O_2	15.495	3.1943	0.0133	0.0065	0.273	0.958	0.614	0.41274	0.570	0.1417	0.909
H_2SO_4	74.356	92.215	0.0012	0.0017	0.806	0.948	0.117	0.00678	0.916	0.1221	0.946
NaOH	11.259	8.7277	0.0037	0.0044	0.574	0.925	0.132	0.12895	0.681	0.1959	0.935

Q_m: maximum adsorption capacity; *b* or K_L: constant related to the strength of interaction adsorbent/adsorbate; R_L: Langmuir constant; R^2: coefficient of determination; K_f: related to the adsorption capacity; *n:* related to the solid heterogeneity; *SE:* standard error.

Table 8. Parameters of the linear mathematical model of Dubinin-Radushkevich (D-R) related to adsorption of Cd^{2+}, Pb^{2+} and Cr^{3+} on *Euterpe Oleracea* endocarp (CA) fresh and modified with H_2O_2, H_2SO_4 and NaOH.

	Fresh CA	CA H_2O_2	CA H_2SO_4	CA NaOH	Fresh CA	CA H_2O_2	CA H_2SO_4	CA NaOH	Fresh CA	CA H_2O_2	CA H_2SO_4	CA NaOH
	---------- Cd^{2+} ----------				---------- Pb^{2+} ----------				---------- Cr^{3+} ----------			
Qd	0.000	$0.2e^{-3}$	0.00037	0.0021	0.000	0.0003	0.00046	0.0007	0.000	$6e^{-05}$	0.00027	0.0044
E	12.328	10.624	13.2686	7.3721	9.704	10.292	10.0707	8.5436	16.440	13.921	15.2854	6.5288
R^2	0.798	0.996	0.997	0.980	0.841	0.995	0.962	0.942	0.838	0.781	0.252	0.826

Q_d: maximum adsorption capacity; *E*: mean sorption energy; R^2: coefficient of determination.

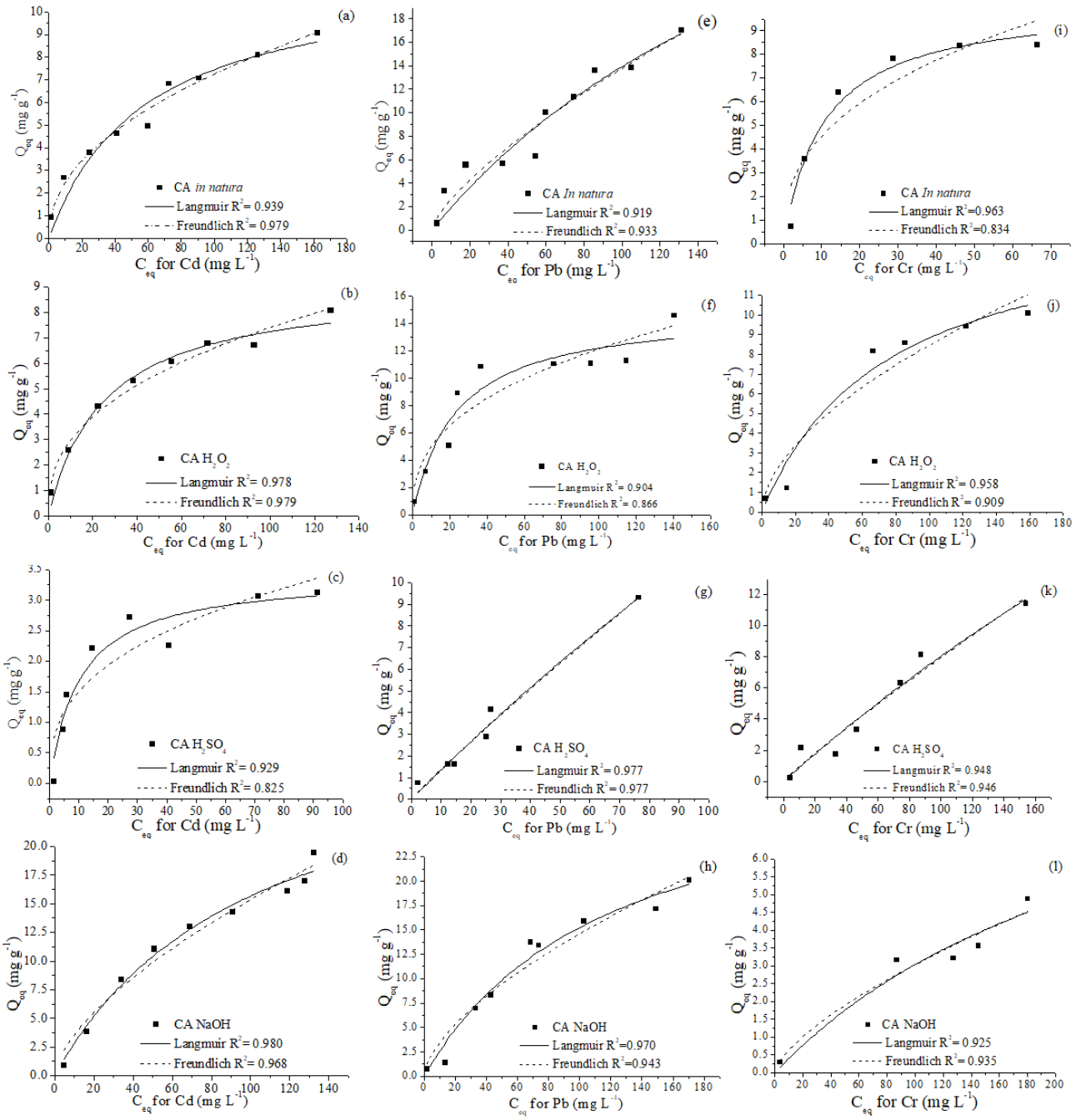

Figure 11. Langmuir and Freundlich adsorption isotherms for sorption of Cd^{2+} (a, b, c, d), Pb^{2+} (e, f, g, h) and Cr^{3+} (i, j, k, l), respectively, by CA fresh and modified with H_2O_2, H_2SO_4 and NaOH.

The Q_m for Cd^{2+} adsorption followed the sequence CA NaOH > fresh CA > CA H_2O_2 > H_2SO_4, with values of 31.714, 11.751, 9.097, and 3.414 mg g^{-1}, respectively. These results corroborate to those found by isotherms (Figure 10). The high adsorption of Pb^{2+} on CA fresh and chemically modified followed the sequence: CA H_2SO_4 (81.197 mg g^{-1}) > fresh CA (47.461 mg g^{-1}) > CA NaOH (33.533 mg g^{-1}) > CA H_2O_2 (15.011 mg g^{-1}), but these values exceed those found by isotherms graphs (Figure 10).

According to Conradi Jr. et al. (2019) Pb^{2+} has strong affinity with carboxyl groups in the adsorbent surface which may explain the high Q_m value obtained in relation to other ions. The sequence of Q_m for Cr^{3+} was greater for CA H_2SO_4 > CA H_2O_2 > CA NaOH > fresh CA, being, respectively, 74.356, 15.495, 11.259 and 10.235 mg g^{-1}.

The parameter b or K_L expresses the strength of interaction between adsorbent and adsorbate, in this case, low values of b (Table 7) show low binding energy among ions of Cd^{2+}, Pb^{2+} and Cr^{3+} and CA fresh and chemically modified with H_2O_2, H_2SO_4 and NaOH, i.e., low affinity/selectivity of the metal-ligand interaction, suggesting that these ions could be readily released in solution.

The reactivity of active sites of the adsorbent can be expressed by the parameter *n* of Freundlich, which is related to the solid heterogeneity. In this study, these values were below one. When the *n* values are close to one, there is a strong indication of the presence of high-energy sites, as observed by Pb^{2+} and Cr^{3+} on CA H_2SO_4. These values can also suggest the occurrence of cooperative adsorption, which involves strong interactions among the molecules of the adsorbate (Schwantes et al., 2018a).

The linear model of D-R describes the adsorption isotherms of systems with individual ions and it was applied in this study (Table 8) to determine the nature of the adsorption process, chemical or physical (Schwantes et al., 2018b).

According to Conradi Jr. et al. (2019), the mean sorption energy (*E*) and D-R is involved in the transfer of 1 mol solute from the solution to the surface of the adsorbent. If the *E* value > 8 kJ mol^{-1}, there is a predominance of chemical adsorption, however, if *E* < 8 kJ mol^{-1}, the nature of the process is physical. In this case, Table 8 indicates that there was predominance of chemical adsorption of Cd^{2+} on the CA H_2O_2 and CA H_2SO_4 modified adsorbents, and for Pb^{2+} on the adsorbents CA H_2O_2, CA H_2SO_4 and CA NaOH. Also, it is observed physical adsorption for Cd^{2+} on CA NaOH. The ion Cr^{3+} showed poor adjustments for the modified adsorbents.

Thermodynamics of adsorption

The nature of the adsorption process can be evaluated by thermodynamic parameters (Gonçalves Jr. et al., 2016). As can be seen in Table 9, the ΔG value for Cd^{2+} on CA H_2O_2, Cr^{3+} on CA H_2O_2 and CA H_2SO_4 was positive for all studied temperatures, suggesting that the process, in this case, is spontaneous and favorable.

The opposite was observed for Pb^{2+} on CA H_2O_2 and Cr^{+3} on CA NaOH. For Cd^{2+} on CA NaOH and for Pb^{2+} on CA H_2O_2 and CA NaOH, the system was spontaneous at temperatures of 15 to 25 °C becoming negative at higher temperatures.

In accordance with Gonçalves Jr. (2013a), when the enthalpy values (ΔH) are positive the system is endothermic, as observed for ions Cd^{2+} and Pb^{2+}. In turn, the negative values of ΔH for Cr^{3+} show that the process was exothermic (Table 9).

Table 9. Values of Q_{eq} and thermodynamic parameters of adsorption for Cd^{2+}, Pb^{2+}, Cr^{3+} on fresh *açaí* endocarp (CA) and chemically modified with H_2O_2, H_2SO_4 and NaOH.

	Temp. °C	Cd^{2+}					Pb^{2+}					Cr^{3+}				
		Q_{eq}	ΔG	ΔH	ΔS	R^2	Q_{eq}	ΔG	ΔH	ΔS	R^2	Q_{eq}	ΔG	ΔH	ΔS	R^2
	15	3.01	-0.003				2.22	-0.010				0.52	0.013			
	25	3.44	-0.003				2.07	-0.010				0.55	0.014			
Fresh CA	35	3.52	-0.004	8.13e^{-6}	0.011	0.990	2.04	-0.010	5.20e^{-6}	0.034	0.92	0.58	0.014	-6.68	0.046	0.963
	45	3.55	-0.004				2.03	-0.011				0.59	0.015			
	55	3.67	-0.004				2.03	0.011				0.60	0.015			
	15	4.97	4.3				0.72	-3.2				6.8	1.6			
	25	5.38	4.4				5.31	-4.5				7.5	2.2			
CA. H_2O_2	35	4.79	4.4	2.35	-6.75	0.983	9.86	-5.7	32.9	125.5	0.986	7.2	2.8	-15.9	-60.8	0.972
	45	5.38	4.5				5.28	-7.0				5.8	3.4			
	55	5.37	4.6				2.53	-8.2				5.9	4.0			
	15	0.72	9.7				7.22	9.7				3.6	4.7			
	25	3.91	6.1				8.28	4.8				4.1	5.4			
CA. H_2SO_4	35	6.92	2.5	112.31	356.4	0.967	10.16	-0.2	152.7	496.3	0.987	3.1	6.1	-15.3	-69.6	0.724
	45	0.66	-1.0				0.46	-5.2				3.1	6.8			
	55	0.10	-4.6				6.42	-10.1				3.8	7.5			
	15	9.68	0.5				11.68	2.7				11.3	-2.3			
	25	9.80	0.1				11.05	1.3				11.7	-2.8			
CA. NaOH	35	9.08	-0.4	13.87	46.3	0.997	12.27	-0.1	42.9	139.8	0.388	11.7	-3.3	12.5	51.5	0.965
	45	11.01	-0.8				10.22	-1.5				11.9	-3.9			
	55	10.71	-1.3				11.36	-2.9				11.4	-4.4			

Q_{eq}: absorbed amount per adsorbent unit (mg g^{-1}); Δ*G*: Gibbs free energy (KJ mol^{-1}); Δ*H*: variation of enthalpy (KJ mol^{-1}); Δ*S*: variation of entropy (J mol^{-1} K^{-1}).

The results in Table 9 still show ΔH values greater than 40 kJ mol^{-1}. These results suggest possible chemisorption for Cd^{2+} on CA H_2SO_4 (112.31 KJ mol^{-1}), and for Pb^{2+} on CA H_2SO_4 (152.7 KJ mol^{-1}) and CA NaOH (42.9 KJ mol^{-1}), and physisorption for Cd^{2+} on CA H_2O_2 and CA NaOH, Pb^{2+} on CA H_2O_2 and Cr^{3+} on all modified adsorbents.

In case of positive entropy values (ΔS), as observed for Cd^{2+} on H_2SO_4 and CA NaOH, for Pb^{2+} on all modified adsorbents and Cr^{3+} on CA NaOH (Table 9), it is suggested an increase on system disorder. In these cases, according to Farghali et al. (2013), there is an increasing disorder of the solid-solution interface, indicating an increased randomness at the solid/solution interface, which may occur due to the substitution of water molecules of the solution previously adsorbed by ion metals.

Conclusion

In general, the adsorbents from *Euterpe Oleracea* endocarp chemically modified with NaOH, H_2SO_4 and H_2O_2 showed differences in structure, morphology, porosity, point of zero charge and thermal stability. The pH had little influence on the adsorption tests and 200 mg (4 g L^{-1}) of adsorbent dose present the highest rates of adsorption. The equilibrium time observed was 40 min, indicating that the adsorption process is fast and can be feasible in larger scale.

The adsorption of toxic metals by *Euterpe Oleracea* based adsorbents proved to be a complex process, occurring both in mono and multilayer, with predominance of monolayer adsorption, and with physical and chemical adsorption. The chemical modification of *Euterpe Oleracea* endocarp with NaOH, H_2SO_4 and H_2O_2 increased the efficiency of this adsorbent in removing Cd^{2+}, Pb^{2+} and Cr^{3+} from aqueous solutions.

Acknowledgements

To CNPq for financial support and for the Research Productivity Fellowship. Also to Capes, since this study was financed in part by the *Coordenação de Aperfeiçoamento de Pessoal de Nível Superior* - Brasil (Capes) - Finance Code 001.

References

Barrett, E. P., Joyner, L. G., & Halenda, P. P. (1951). The determination of pore volume and area distributions in porous substances. I. Computations from nitrogen isotherms. *Journal of American Chemistry Society, 73*(1), 373-380. doi: 10.1021/ja01145a126

Barros, N. B., Bruns, R. E., Scarminio, I. S. (2010). *How do experiments: Applications in science and industry* (4th ed.) New York: Bookman.

Bartczak, P., Norman, M., Klapiszewski, Ł., Karwańska, N., Kawalec, M., Baczyńska, M., ... Jesionowski, T. (2018). Removal of nickel(II) and lead(II) ions from aqueous solution using peat as a low-cost adsorbent: A kinetic and equilibrium study. *Arabian Journal of Chemistry, 11*(8), 1209-1222. doi: 10.1016/j.arabjc.2015.07.018

Bohli, T., Ouederni, A., Fiol, N., & Villaescusa, I. (2015). Evaluation of an activated carbon from olive stones used as an adsorbent for heavy metal removal from aqueous phases. *Comptes Rendus Chimie, 18*(1), 88-99. doi: 10.1016/j.crci.2014.05.009

Brunauer, S., Emmett, P. H., & Teller, E. (1938). Adsorption of gases in multimolecular layers. *Journal of American Chemistry Society, 60*(2), 309-319.

Chazin, E. L. (2012). Preparation methods of industrial solvents and chemical reagents. *Revista Virtual de Química, 4*(6), 872-883. doi: 10.5935/1984-6835.20120061

Coelho, G. F., Gonçalves Jr., A. C., Tarley, C. R. T., Casarin, J., Nacke, H., & Francziskowski, M. A. (2014). Removal of metal ions Cd (II), Pb (II), and Cr (III) from water by the cashew nut shell *Anacardium occidentale* L. *Ecological Engineering, 73*, 514-525. doi: 10.1016/j.ecoleng.2014.09.103

Conradi Jr., E., Gonçalves Jr., A. C., Schwantes, D., Manfrin, J., Schiller, A. P., Zimmerman, J., ... Ziemer, G. L. (2019). Development of renewable adsorbent from cigarettes for lead removal from water. *Journal of Environmental Chemical Engineering, 7*(4), 103200-103262. doi: 10.1016/j.jece.2019.103200

Cutillas-Barreiro, L., Ansias-Manso, L., Fernández-Calviño, D., Arias-Estévez, M., Nóvoa-Muñoz, J. C., Fernández-Sanjurjo, M. J., ... Núñez-Delgado, A. (2014). Pine Bark as bio-adsorbent for Cd, Cu, Ni, Pb and Zn: Batch-type and stirred flow chamber experiments. *Journal of Environmental Management, 114*, 258-264. doi: 10.1016/j.jenvman.2014.06.008

Dubinin, M. M., & Radushkevich, L. V. (1947). The equation of the characteristic curve of the activated charcoal. *Union of Soviet Socialist Republics Academy of Sciences*, *55*, p. 331-337.

Ercan, Ö., & Aydin, A. (2013). Removal of mercury, antimony, cadmium and lead from aqueous solution using 1,3,5-trithiane as an adsorbent. *Journal of the Brazilian Chemical Society, 24*(5), 865-872. doi: 10.5935/0103-5053.20130114

Farghali, A. A., Bahgat, M., El Rouby, W. M. A., & Khedr, M. H. (2013). Preparation, decoration and characterization of graphene sheets for methyl green adsorption. *Journal of Alloys and Compounds, 555*, 193-200. doi: 10.1016/j.jallcom.2012.11.190

Freundlich, H. M. F. (1906). Over the adsorption in solution. *The Journal of Physical Chemistry, 57*, 385-471.

Giles, C. H., MacEwan, T. H., Nakhwa, S. N., & Smith, D. (1960). Studies in adsorption. Part XI. A system of classification of solution adsorption isotherms, and its use in diagnosis of adsorption mechanisms and in measurement of specific surface areas of solids. *Journal of the Chemical Society*, 3973-3993.

Gonçalves Jr., A. C., Coelho, G. F., Schwantes, D., Rech, A. L., Campagnolo, M. Â., & Miola, A. Jr. (2016). Biosorption of Cu (II) and Zn (II) with açaí endocarp *Euterpe oleracea* M. in contaminated aqueous solution. *Acta Scientiarum. Technology, 38*(3), 361-370. doi: 10.4025/actascitechnol.v38i3.28294

Gonçalves Jr., A. C., Meneghel, A. P., Rubio, F., Strey, L., Dragunski, D. C., & Coelho, G. F. (2013a). Applicability of *Moringa oleifera* Lam. pie as an adsorbent for removal of heavy metals from waters. *Revista Brasileira de Engenharia Agrícola e Ambiental, 17*(1), 94-99. doi: 10.1590/S1415-43662013000100013

Gonçalves Jr., A. C., Rubio, F., Meneghel, A. P., Coelho, G. F., Dragunski, D. C., & Strey, L. (2013b). The use of *Crambe abyssinica* seeds as adsorbent in the removal of metals from waters. *Revista Brasileira de Engenharia Agrícola e Ambiental, 17*(3), 306-311. doi: 10.1590/S1415-43662013000300009

Ho, Y. S., & McKay, G. (1999). Pseudo-second order model for sorption process. *Process Biochemistry, 34*(5), 451-465. doi: 10.1016/S0032-9592(98)00112-5

Khandaker, S., Toyohara, Y., Kamida, S., & Kuba, T. (2018). Adsorptive removal of cesium from aqueous solution using oxidized bamboo charcoal. *Water Resources and Industry, 19*, 35-46. doi: 10.1016/j.wri.2018.01.001

Kiran, B. M., Srikantaswamy, S., Pallavi, H. V., Manoj, V., & Tasneem, T. (2013). A Study on utilization of Groundnut Shell as biosorbent for Heavy metals removal. *Journal of Environmental Science, Computer Science and Engineering & Technology, 2*(1), 173-186.

Lagergren, S. (1898). Zur theorie der sogenannten adsorption geloster stoffe. *Kungliga Svenska Vetenskapsakademiens Handlingar, 24*(4), 1-39.

Langmuir, I. (1916). The constitution and fundamental properties of solids and liquids. Part I. Solids. *Journal of the American Chemical Society, 38*(11), 2221-2295.

Latimer, G. W. Jr. (2012). *Official methods of analysis* (19th ed.). Maryland, MD: AOAC.

Melzer, M., Blin, J., Bensakhria, A., Valette, J., & Broust, F. (2013). Pyrolysis of extractive rich agroindustrial residues. *Journal of Analytical and Applied Pyrolysis, 104*, 448-460. doi: 10.1016/j.jaap.2013.05.027

Meneghel, A. P., Gonçalves Jr., A. C., Strey, L., Rubio, F., Schwantes, D., & Casarin, J. (2013). Biosorption and removal of chromium from water by using moringa seed cake (*Moringa oleifera* Lam.). *Química Nova, 36*(8), 1104-1110. doi: 10.1590/S0100-40422013000800005

Mimura, A. M. S., Vieira, T. V. A., Martelli, P. B., & Gorgulho, H. F. (2010). Utilization of rice husk to remove Cu^{2+}, Al^{3+}, Ni^{2+} and Zn^{2+} from wastewater. *Química Nova, 33*(6), 1279-1284. doi: 10.1590/S0100-40422010000600012

Moreira, R., Orsini, R. R., Vaz, J. M., Penteado, J. C., & Spinacé, E. V. (2016). Production of biochar, bio-oil and synthesis gas from cashew nut shell by slow pyrolysis. *Waste and Biomass Valorization, 8*, 217-224. doi: 10.1007/s12649-016-9569

Movasaghi, Z., Rehman, S., & Rehman, I. (2008). Fourier Transform Infrared (FTIR) spectroscopy of biological tissues. *Applied Spectroscopy Reviews, 43*(2), 134-179. doi: 10.1080/05704920701829043

Nacke, H., Gonçalves Jr., A. C., Campagnolo, M. A., Coelho, G. F., Schwantes, D., Santos, M. G., ... Zimmermann, J. (2016). Adsorption of Cu (II) and Zn (II) from Water by *Jatropha curcas* L. as biosorbent. *Open Chemistry, 14*(1), 103-177. doi: 10.1515/chem-2016-0010

Nacke, H., Gonçalves Jr., A. C., Coelho, G. F., Schwantes, D., Campagnolo, M. A., Leismann, E. A. V., ... Miola, A. J. (2017). Removal of Cd (II) from water using the waste of jatropha fruit (*Jatropha curcas* L.). *Applied Water Science, 7*, 3207-3222. doi: 10.1007/s13201-016-0468-2

Nascimento, W. M. O., Cicero, S. M., & Novembre, A. D. L. C. (2010). Conservação de sementes de açaí (*Euterpe oleracea* Mart.). *Revista Brasileira de Sementes, 32*(1), 24-33.

Oliveira, L. S., & Franca, A. S. (2011). Conventional and non-conventional thermal processing for the production of activated carbons from agro-industrial wastes. *Activated Carbon: Classifications, Properties and Applications, 11*, 205-238.

Pacheco-Palencia, L. A., Duncan, C. E., & Talcott, S. T. (2009). Phytochemical composition and thermal stability of two commercial acai species, *Euterpe oleracea* and *Euterpe precatoria*. *Food Chemistry, 115*(4), 1199-1205. doi: 10.1016/j.foodchem.2009.01.034

Pavia, D. L., Lampman, G. M., Kriz, G. S., & Vyvyan, J. R. (2010). Introdução à espectroscopia (4 ed.). São Paulo, SP: Cengage Learning.

Penha, R. S., Santos, C. C., Cardoso, J. J. F., Silva, H. A. S., Santana, S. A. A., & Bezerra, C. W. B. (2016). Chemically treated rice husk as low-cost adsorbent for metal ions uptake (CO^{2+} and Ni^{2+}). *Revista Virtual de Química, 8*(3), 588-604. doi: 10.5935/1984-6835.20160045

Quintáns-Fondo, A., Ferreira-Coelho, G., Paradelo-Núñez, R., Nóvoa-Muñoz, J. C., Arias-Estévez, M., Fernández-Sanjurjo, M. J., ... Núñez-Delgado, A. (2016). As (V)/Cr(VI) pollution control in soils, hemp waste, and other by-products: competitive sorption trials. *Environmental Science and Pollution Research International, 23*(19), 19182-19192. doi: 10.1007/s11356-016-7108-0

Ribeiro, G. A. C., Silva, D. S. A., Santos, C. C., Vieira, A. P., Bezerra, C. W. B., Tanaka, A. A., & Santana, S. A. A. (2017). Removal of remazol brilliant violet textile dye by adsorption using rice hulls. *Polímeros, 27*(1), 16-26. doi: 10.1590/0104-1428.2386

Roginski, S. Z. (1948). Adsorption and catalysis on inhomogeneous surfaces. The Academy of Sciences of the U.S.S.R.. Moscow-Leningrad. 353-455.

Rubio, F., Gonçalves Jr., A. C., Meneghel, A. P., Tarley, C. R. T., Schwantes, D., & Coelho, G. F. (2013a). Removal of cadmium from water using by-product *Crambe abyssinica* Hochst seeds as biosorbent material. *Water Science & Technology, 68*(1), 227-233. doi: 10.2166/wst.2013.233

Rubio, F., Gonçalves Jr., A. C., Strey, L., Meneghel, A. P., Coelho, G. F., & Nacke, H. (2013b). Applicability of *Crambe abyssinica* Hochst. byproduct as biosorbent in the removal of chromium from water. *Spanish Journal of Rural Development, 4*(1), 25-40. doi: 10.5261/2013.GEN1.03

Schiller, A. P., Ferronato, M. C., Schwantes, D., Gonçalves Jr., A. C., Barilli, D. J., & Manfrin, J. (2019). Influence of hydrological flows from tropical watersheds on the dynamics of Cu and Zn in sediments. *Environmental Monitoring and Assessment, 191*(2), 86. doi: 10.1007/s10661-019-7193-x

Schwantes, D., Gonçalves Jr., A. C., Campagnolo, M. A., Tarley, C. R. T., Dragunski, D. C., Varennes, A., ... Conradi Jr., E. (2018a). Chemical modifications on pinus bark for adsorption of toxic metals. *Journal of Environmental Chemical Engineering, 6*(1), 1271-1278. doi: 10.1016/j.jece.2018.01.044

Schwantes, D., Gonçalves Jr., A. C., Coelho, G. F., Campagnolo, M. A., Dragunski, D. C., Tarley, C. R. T., ... Leismann, E. A. V. (2016). Chemical modifications of cassava peel as adsorbent material for metals ions from wastewater. *Journal of Chemistry, 2016*, 1-15. doi: 10.1155/2016/3694174

Schwantes, D., Gonçalves Jr., A. C., Coelho, G. F., Campgnolo, M. A., Santos, M. G., Miola, A. Jr., & Leismann, E. A. V. (2015). Crambe pie modified for removal chromiumfromaqueous solution. *International Journal of Current Research, 7*(10), 21658-21669.

Schwantes, D., Gonçalves Jr., A. C., Schiller, A. P., Manfrin, J., Campagnolo, M. A., & Somavilla, E. (2019). *Pistia stratiotes* in the phytoremediation and post-treatment of domestic sewage. *International Journal of Phytoremediation, 21*(7), 714-723. doi: 10.1080/15226514.2018.1556591

Schwantes, D., Gonçalves Jr., A. C., Strey, L., Schwantes, V., & Nacke, H. (2013). Reuse and recycling techniques: Kinetics, equilibrium and thermodynamics of the adsorption process of lead using cassava industry wastes. In H. Bartolo, P. J. S. Bartolo, N. M. F. Alves, A. J. Mateus, H. A. Almeida, A. C. S. Lemos, ... J. P. Neves (Eds.), *Green design, materials and manufacturing processes* (p. 417-422). Boca Raton, FL: CRC Press.

Schwantes, D., Gonçalves Jr., A. C., Varennes, A., & Braccini, A. L. (2018b). Modified grape stem as a renewable adsorbent for cadmium removal. *Water Science and Technology, 78*(11), 2308-2320. doi: 10.2166/wst.2018.511

Smidt, E., & Meissl, K. (2007). The applicability of Fourier transform infrared (FT-IR) spectroscopy in waste management. *Waste Management, 27*(2), 268-276. doi: 10.1016/j.wasman.2006.01.016

Sun, C.-J., Sun, L.-Z., & Sun, X.-X. (2013). Graphical evaluation of the favorability of adsorption processes by using conditional langmuir constant. *Industrial & Engineering Chemistry Research, 52*(39), 14251-14260. doi: 10.1021/ie401571p

Weber, W. J., Morris, J. C. (1963). Kinetics of adsorption on carbon from solution. *Journal of Sanitary Engineering Division ASCE*, *89*(2), 31-60.